



**COMILLAS**  
UNIVERSIDAD PONTIFICIA

ICAI

BACHELOR'S DEGREE IN ENGINEERING  
FOR INDUSTRIAL TECHNOLOGIES

BACHELOR'S FINAL PROJECT

WIND UNCERTAINTY WHEN PROVIDING  
PRIMARY FREQUENCY CONTROL

Author: Rodríguez Barrero, Gonzalo Manuel

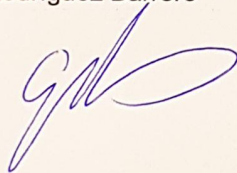
Director: Sigrist, Lukas

Madrid  
June 2023

Declaro, bajo mi responsabilidad, que el Proyecto presentado con el título  
"Wind uncertainty when providing primary frequency control"  
en la ETS de Ingeniería - ICAI de la Universidad Pontificia Comillas en el  
curso académico 2022-2023 es de mi autoría, original e inédito y  
no ha sido presentado con anterioridad a otros efectos. El Proyecto no es  
plagio de otro, ni total ni parcialmente y la información que ha sido tomada  
de otros documentos está debidamente referenciada.

Fdo.: Gonzalo Manuel Rodríguez Barrero

Fecha: 24 / 06 / 2023




Autorizada la entrega del proyecto

EL DIRECTOR DEL PROYECTO

Fdo.: Lukas Sigríst

Fecha: 26 / 06 / 2023





**COMILLAS**  
UNIVERSIDAD PONTIFICIA

ICAI

BACHELOR'S DEGREE IN ENGINEERING  
FOR INDUSTRIAL TECHNOLOGIES

BACHELOR'S FINAL PROJECT

WIND UNCERTAINTY WHEN PROVIDING  
PRIMARY FREQUENCY CONTROL

Author: Rodríguez Barrero, Gonzalo Manuel

Director: Sigrist, Lukas

Madrid  
June 2023

---

# WIND UNCERTAINTY WHEN PROVIDING PRIMARY FREQUENCY CONTROL

Author: Rodríguez Barrero, Gonzalo Manuel

Director: Sigrist, Lukas

Collaborating Entity: ICAI - Universidad Pontificia Comillas.

## ABSTRACT

Ensuring grid frequency stability is crucial, especially in island power systems that are more vulnerable to frequency fluctuations due to their low inertia. As more renewable energies are integrated, such as Wind Generators (WGs), which do not contribute inertia to the system, the stability of the power system is reduced in cases of accidental disconnection of conventional Generators (CGs) during drops in wind speed. This project focuses on modelling the WGs, the power system with WGs and analysing simulations with different wind characteristics and losses of CGs. The results show that the provision of Primary Frequency Regulation (PFR) does not significantly improve stability in situations of reduced wind speed, and that increased wind penetration and decreased wind speed negatively affect system stability, especially when they occur simultaneously with the loss of CGs.

Keywords: Primary Frequency Regulation, Wind Generators

## Introduction

Ensuring frequency stability of the grid is of great importance. If this frequency falls below a certain threshold, load will have to be disconnected so as to improve the system's ability to maintain an equilibrium between the system's generation and load [1]. This disconnection is carried out with an Under-Frequency Load Shedding (UFLS) scheme. This stability is determined by the inertia of the primer movers, generators and their respective primary frequency regulation [2]. Island systems are small and isolated, which means they have low inertia in their system. This makes them particularly vulnerable to frequency fluctuations. Meanwhile, the world is integrating more renewables into the grid. For example, the European Union (EU) has nearly doubled its wind energy capacity from 2012 to 2021 [3]. However, WGs are connected through power converters that mechanically decouple them from the grid, thus not attaching inertia to the system. This replacement of CGs with WGs reduces the stability of the power system.

WGs may offer different ways to offer such a primary frequency regulation. Two of the most conventional methods is through the rotor speed and the pitch angle control [4]. They allow the WG to operate at the desired power and rotor speed combination. Normally, WGs operate at a Maximum Power Point (MPP), that is, they always provide

---

the maximum power given the circumstantial wind speed. However, these controls may be used so that they operate at a deloaded operation mode. This intentionally makes the WG provide less power so that, when a frequency event comes (e.g. the loss of a generator), they can partially compensate the imbalance between the generation and load. This extra power added is controlled by the droop control, which responds to frequency deviation.

The mechanical power of a wind turbine can be expressed by [5, 6, 7]:

$$P_m = \frac{1}{2} \rho A_w c_p(\lambda, \theta) v_w^3 \quad (1)$$

Where  $P_m$  is the mechanical power (in  $W$ ),  $\rho$  is the air density (in  $kg/m^3$ ),  $A_w$  is the area swept by the blades (in  $m^2$ ),  $c_p$  is the performance coefficient,  $v_w$  is the wind speed (in  $m/s$ ) and  $\lambda$  is the tip speed ratio:

$$\lambda = \frac{\omega_r R}{v_w} \quad (2)$$

Where  $R$  is the radius of the blades and  $\omega_r$  is the rotor speed. These equations give a numerical approximation of the relationship between the mechanical power and the incoming wind speed. It also enables one to relate the rotor speed  $\omega_r$  and the pitch angle  $\theta$  to the mechanical power obtained. However, the electrical power, not the mechanical one, is of concern when it comes to the power system's imbalances. It is possible to relate them [5, 8]:

$$T_m - T_e = 2H \frac{d\omega_r}{dt} \quad (3)$$

These equations can be combined so that a WG model is built. This model can be then integrated into a System Frequency Dynamics (SFD) model where the main assumption is that the frequency of the grid is uniform [2]. Additionally, the CGs are represented by a state-space and saturation. The combination of these components allow the analysis of a power grid with high wind energy penetration.

The objective of this project is to analyse how different wind-related parameters may affect the frequency stability at the time of a CG loss. For this purpose, a WG will be modelled, integrated into a power system model, and then the system will be simulated with different parameters. MATLAB/Simulink software is used for the modelling and for the time-domain simulations.

## Methodology

From Equation 1, the relationship between the rotor speed, the mechanical power and the Maximum Power Point Tracking (MPPT) and deloaded curves can be plotted, as shown in Figure 1. An initial generation power is given and the corresponding equilibrium position within the deloaded curve is set.

The control implemented follows the deloaded curve when the wind speed changes. However, when a frequency event occurs, the control will shift its operation point

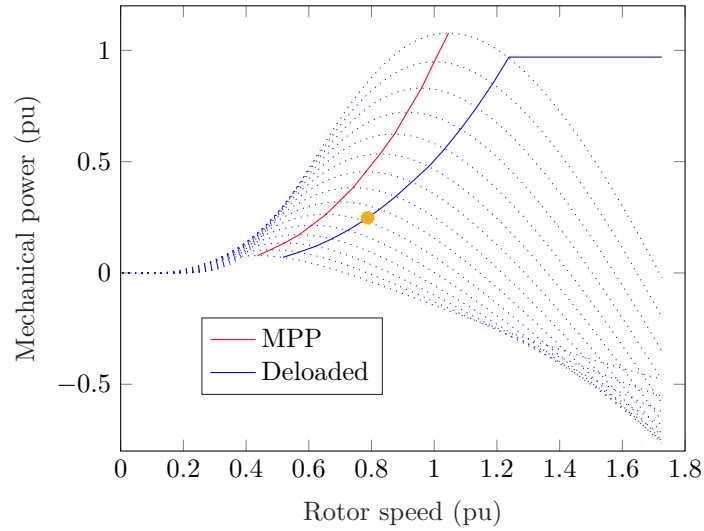


Figure 1: Power-speed plot. The yellow dot represents an operating point in equilibrium at a deloaded operation mode.

towards the MPP given the current wind speed. This “shift” is realised by the provision of additional active power by the droop controller.

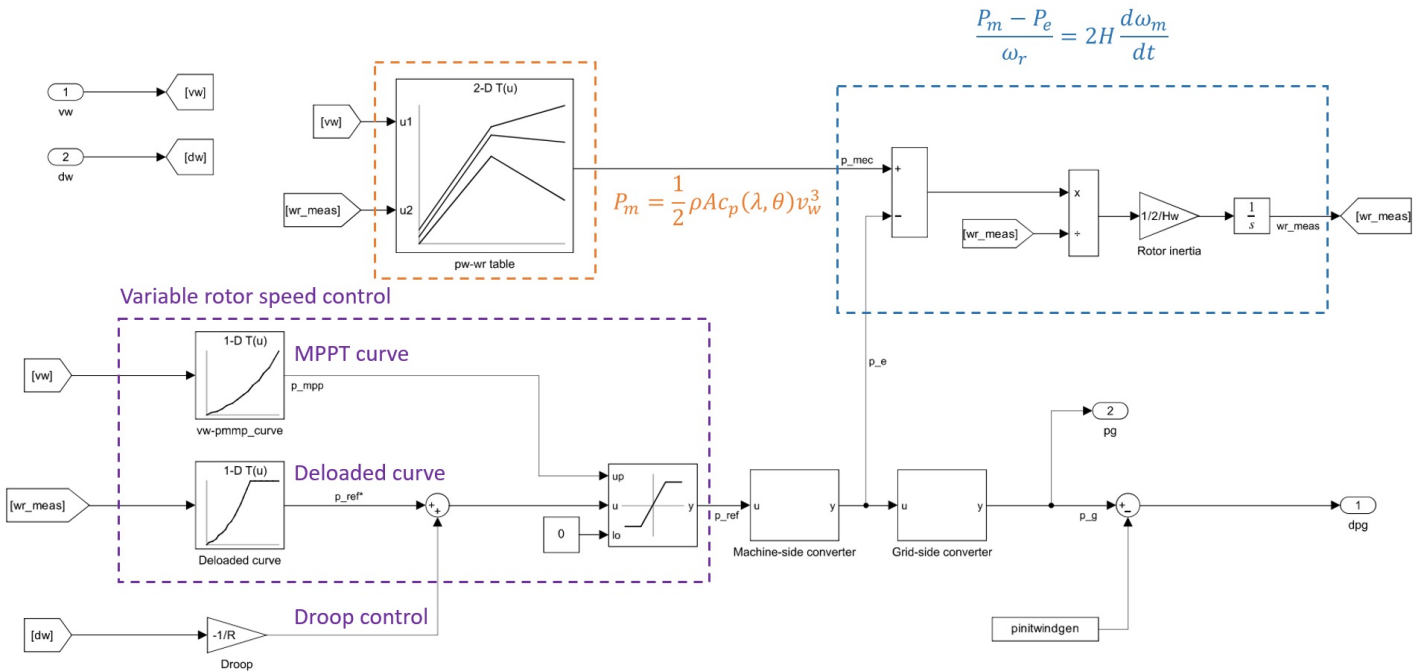


Figure 2: WG model in Simulink.

The Simulink model of the WG is represented in [Figure 2](#). It takes into account [Equation 1](#) for obtaining the mechanical power from the measured rotor speed. It uses the deloaded curve from [Figure 1](#) to set the reference power. The MPPT curve from the same figure is used to know the saturation of the droop point added to the reference

power  $P_{ref*}$ . This outputted power, when gone through the machine-side converter, turns into the actual electrical power that the WG provides.

Then the WGs can be integrated into the power system by placing them in parallel and connecting them depending on the desired wind energy penetration.

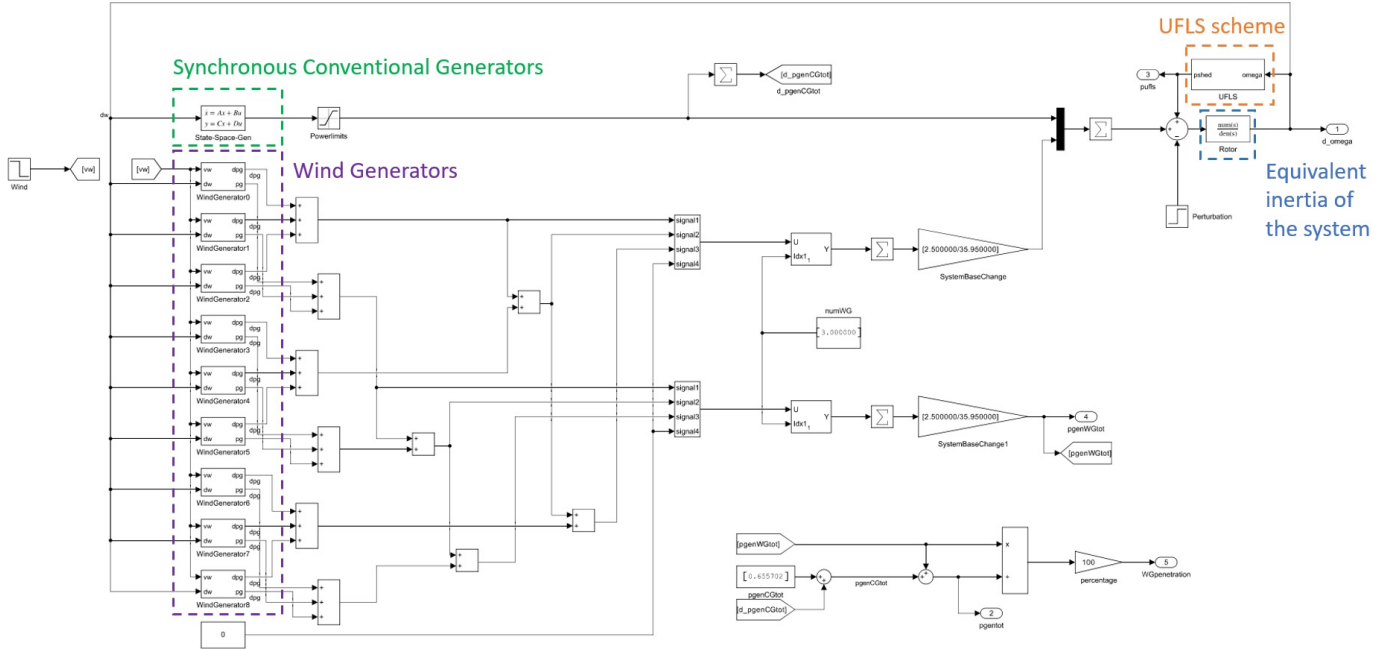


Figure 3: Powersystem model in Simulink.

The steady-state frequency and the power load shedded by the UFLS scheme can be obtained by simply taking the last element of the array that is outputted from the simulation. On the other hand, the nadir frequency is obtained by looking for the minimum value in this same array with frequency values.

## Results

The impact of the number of WGs, variations in wind speed, and the timing of these changes can be quantified. One way to assess this is by respectively summing all the total shed load and the maximum frequency deviation across all simulations, focusing on each specific parameter. The results are presented on [Table 1](#), [Table 2](#), and [Table 3](#).

It can be seen that as the WG penetration becomes larger, both the deviation from the nominal frequency and the shed load becomes greater. This proves that generally speaking, when more WGs are connected to the system, it becomes less stable. It follows from [Table 2](#) that as the wind speed change becomes greater, so does the instability of the system. Nonetheless, [Table 3](#) shows that the timing at which the wind change happens is not as significant, however its impact is greatest when the wind changes at the same time as the frequency event.

Table 1: Sums of the shed power and maximum deviations from the base frequency from all simulations, depending on number of WGs in the system.

	3 WGs	6 WGs	9 WGs
$\Sigma P_{ufls}$	2172.1	2408.2	2617.5
$\Sigma \Delta f_{min}$	1450.4	1468.4	1504.7

Table 2: Sums of the shed power and maximum deviations from the base frequency from all simulations, depending on the wind speed change.

	0 m/s	0.5 m/s	1 m/s
$\Sigma P_{ufls}$	2084.5	2327.5	2785.8
$\Sigma \Delta f_{min}$	1338.9	1479.9	1604.6

Table 3: Sums of the shed power and maximum deviations from the base frequency from all simulations, depending on the time of the wind speed change.

	-2 s	0 s	+2 s
$\Sigma P_{ufls}$	2381.8	2470.8	2345.2
$\Sigma \Delta f_{min}$	1486.6	1502.0	1434.8

## Conclusions

Upon analyzing the cumulative total demand shed and frequency deviations across all conceivable simulations, a clear pattern emerges. As the number of integrated WGs increases, the system experiences heightened instability. Similarly, as the wind speed change increases, the system becomes increasingly unstable, as expected. However, the precise timing of the wind speed drop proves to be less influential compared to other parameters. Nevertheless, a more critical level is reached when the wind speed drops simultaneously with a frequency event.

The implemented control action in this project solely reacts to changes in wind speed and frequency deviation. It would be highly valuable to introduce a control mechanism aimed at increasing power output during inevitable reductions. In cases where a frequency event transpires while operating in a deloaded mode with a constant wind speed, the rotor speed decelerates. However, following the deloaded operation mode, the power output would naturally decrease.

This project can also be improved by including a pitch angle controller or stall control into the WG model. Additionally, the use of a discretized model with a sample frequency and the addition of noise could make the rotor speed measurement assumptions more realistic. Allowing for variances across various WGs and taking into account various wind patterns could enhance wind modeling. Investigating the Rate of Change of Frequency (ROCOF) and taking into account additional grid stability indicators may be further analysed. It would be difficult to weigh various stability indicators, but doing so might result in a more thorough or holistic analysis.





# Bibliography

- [1] P. Kundur et al. “Definition and classification of power system stability IEEE/CIGRE joint task force on stability terms and definitions”. In: *IEEE Transactions on Power Systems* 19.3 (2004), pp. 1387–1401. DOI: [10.1109/TPWRS.2004.825981](https://doi.org/10.1109/TPWRS.2004.825981).
- [2] L. Sigrist et al. *Island Power Systems*. CRC Press, Taylor & Francis Group, 2016. ISBN: 9781498746380.
- [3] IRENA. *Renewable Capacity Statistics 2022*. Último acceso: 29-06-2023. IRENA, 2022, p. 14. ISBN: 978-92-9260-428-8. URL: <https://www.irena.org/publications/2022/Apr/Renewable-Capacity-Statistics-2022>.
- [4] O. Apata and D.T.O. Oyedokun. “An overview of control techniques for wind turbine systems”. In: *Scientific African* 10 (2020), e00566. ISSN: 2468-2276. DOI: <https://doi.org/10.1016/j.sciaf.2020.e00566>. URL: <https://www.sciencedirect.com/science/article/pii/S2468227620303045>.
- [5] J.G. Slootweg et al. “General model for representing variable speed wind turbines in power system dynamics simulations”. In: *IEEE Transactions on Power Systems* 18.1 (2003), pp. 144–151. DOI: [10.1109/TPWRS.2002.807113](https://doi.org/10.1109/TPWRS.2002.807113).
- [6] Kara Clark, Nicholas W. Miller, and Juan J. Sanchez-Gasca. *Modeling of GE Wind Turbine-Generators for Grid Studies*. Tech. rep. Version 4.5. One River Road, Schenectady, NY 12345, USA: General Electric International, Inc., Apr. 2010. URL: [https://www.researchgate.net/publication/267218696\\_Modeling\\_of\\_GE\\_Wind\\_Turbine-Generators\\_for\\_Grid\\_Studies\\_Prepared\\_by](https://www.researchgate.net/publication/267218696_Modeling_of_GE_Wind_Turbine-Generators_for_Grid_Studies_Prepared_by).
- [7] James F. Conroy and Rick Watson. “Frequency Response Capability of Full Converter Wind Turbine Generators in Comparison to Conventional Generation”. In: *IEEE Transactions on Power Systems* 23.2 (2008), pp. 649–656. DOI: [10.1109/TPWRS.2008.920197](https://doi.org/10.1109/TPWRS.2008.920197).
- [8] Hongtao ma and Badrul Chowdhury. “Working towards frequency regulation with wind plants: Combined control approaches”. In: *Renewable Power Generation, IET* 4 (Aug. 2010), pp. 308–316. DOI: [10.1049/iet-rpg.2009.0100](https://doi.org/10.1049/iet-rpg.2009.0100).

---

# INCERTIDUMBRE DEL VIENTO AL PROPORCIONAR REGULACIÓN PRIMARIA DE FRECUENCIA

Autor: Rodríguez Barrero, Gonzalo Manuel

Director: Sigrist, Lukas

Entidad Colaboradora: ICAI - Universidad Pontificia Comillas.

## RESUMEN DEL PROYECTO

Garantizar la estabilidad de la frecuencia de la red eléctrica es crucial, especialmente en sistemas insulares que son más vulnerables a las fluctuaciones de frecuencia debido a su baja inercia. A medida que se integran más energías renovables, como los Generadores Eólicos (GEs), que no aportan inercia al sistema, se reduce la estabilidad del sistema eléctrico en casos de desconexión accidental de Generadores Convencionales (GCs) durante caídas en la velocidad del viento. Este proyecto se centra en modelar los GEs, el sistema eléctrico con GEs y analizar simulaciones con diferentes características del viento y pérdidas de GCs. Los resultados demuestran que la provisión de Regulación Primaria de Frecuencia (RPF) no mejora significativamente la estabilidad en situaciones de reducción de la velocidad del viento, y que el aumento de la penetración eólica y la disminución de la velocidad del viento afectan negativamente la estabilidad del sistema, especialmente cuando ocurren simultáneamente con la pérdida de GCs.

Palabras clave: Regulación Primaria de Frecuencia, Aerogeneradores

## Introducción

Es de gran importancia garantizar la estabilidad de la frecuencia de la red. Si esta frecuencia cae por debajo de un determinado umbral, se tendrá que desconectar la carga para mejorar la capacidad del sistema de mantener un equilibrio entre la generación y la carga [1] del sistema. Esta desconexión se realiza mediante un deslastre de cargas por subfrecuencia (Under-Frequency Load Shedding (UFLS) en inglés). Esta estabilidad viene determinada por la inercia de los motores primarios, generadores y su respectiva regulación primaria de frecuencia [2]. Los sistemas insulares son pequeños y aislados, lo que significa que tienen una baja inercia en su sistema. Esto los hace especialmente vulnerables a las fluctuaciones de frecuencia. En cambio, el mundo está integrando más energías renovables en la red. Por ejemplo, la Unión Europea (UE) ha prácticamente duplicado su capacidad de energía eólica entre los años 2012 a 2021 [3]. Sin embargo, los aerogeneradores se conectan a través de convertidores de potencia que los desacoplan mecánicamente de la red, por lo que no aportan inercia al sistema. Esta sustitución de generadores síncronos por aerogeneradores reduce la estabilidad del sistema eléctrico.

Un Generador Eólico (GE) puede ofrecer diferentes formas de ofrecer dicha regula-

ción primaria de frecuencia. Dos de los métodos más convencionales son mediante el control de la velocidad del rotor y del ángulo de paso [4]. Permiten que el aerogenerador funcione con la combinación deseada de potencia y velocidad del rotor. Normalmente, los aerogeneradores funcionan a un Punto de Potencia Máxima (Maximum Power Point (MPP) en inglés), es decir, siempre proporcionan la máxima potencia dada la velocidad actual del viento. Sin embargo, estos controles pueden utilizarse de modo que funcionen en un modo de operación deloaded. Este modo de operación hace intencionadamente que el aerogenerador proporcione menos potencia para que, cuando se produzca un evento de frecuencia (por ejemplo, la pérdida de un generador), pueda compensar parcialmente el desequilibrio entre la generación y la demanda. Esta potencia extra añadida se controla mediante el control de estatismo, que responde a la desviación de la frecuencia.

Se puede expresar el comportamiento mecánico de un aerogenerador mediante la siguiente ecuación [5, 6, 7]:

$$P_m = \frac{1}{2} \rho A_w c_p(\lambda, \theta) v_w^3 \quad (1)$$

Siendo  $P_m$  la potencia mecánica (en  $W$ ),  $\rho$  la densidad del aire (en  $kg/m^3$ ),  $A_w$  el área barrida por las palas (en  $m^2$ ),  $c_p$  el coeficiente de rendimiento,  $v_w$  velocidad del viento (en  $m/s$ ) y  $\lambda$  la relación de velocidad de punta:

$$\lambda = \frac{\omega_r R}{v_w} \quad (2)$$

Siendo  $R$  el radio de las palas y  $\omega_r$  la velocidad del rotor. Estas ecuaciones dan una aproximación numérica de la relación entre la potencia mecánica y la velocidad del viento entrante. También permiten relacionar la velocidad del rotor  $\omega_r$  y el ángulo de paso  $\theta$  con la potencia mecánica obtenida. Sin embargo, lo que más importa en cuanto a los desequilibrios del sistema eléctrico es la potencia eléctrica, no la mecánica. Es posible relacionar estas dos potencias mediante [5, 8]:

$$T_m - T_e = 2H \frac{d\omega_r}{dt} \quad (3)$$

Estas ecuaciones pueden juntarse de modo que se forme un modelo de aerogenerador. A continuación, este modelo puede integrarse en un modelo System Frequency Dynamics (SFD) en el que la hipótesis principal es que la frecuencia de la red es uniforme [2]. Además, los Generadores Convencionales (GC) se representan mediante un espacio de estados seguido de una saturación. La combinación de estos componentes permite el análisis de una red eléctrica con alta penetración de energía eólica.

El objetivo de este proyecto es analizar cómo diferentes parámetros relacionados con el viento pueden afectar a la estabilidad de la frecuencia en el momento de una pérdida de un GC. Para ello, se modelará un aerogenerador, se integrará en un modelo de sistema de potencia y, posteriormente, se simulará el sistema con diferentes parámetros. Para el modelado y las simulaciones en el dominio temporal se utiliza el software MATLAB/Simulink.

---

## Metodología

A partir de la [Figura 1](#), se puede trazar la relación entre la velocidad del rotor, la potencia mecánica y las curvas Maximum Power Point Tracking (MPPT) y deloaded, como se muestra en la [Figura 1](#). Se da una potencia de generación inicial y se establece la posición de equilibrio correspondiente dentro de la curva deloaded.

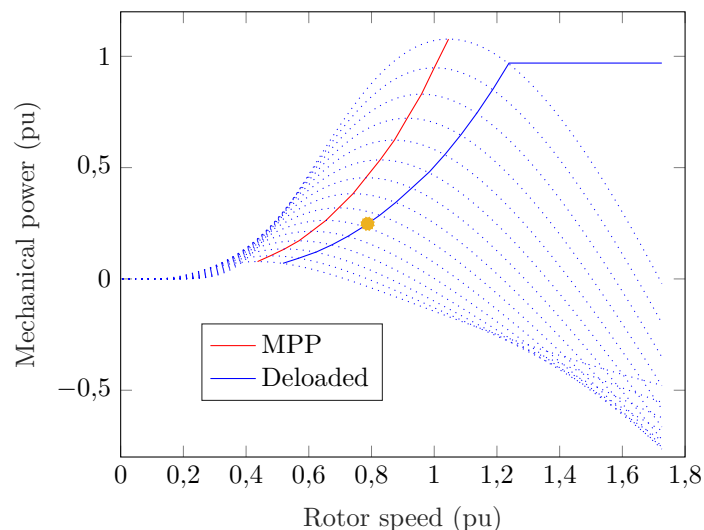


Figura 1: Gráfico potencia-velocidad. El punto amarillo representa un punto de funcionamiento en equilibrio en un modo de operación deloaded.

El control implementado sigue la curva deloaded cuando cambia la velocidad del viento. Sin embargo, cuando se produce un evento de frecuencia, el control desplazará su punto de funcionamiento hacia el MPP dada la velocidad actual del viento. Este “desplazamiento” se realiza mediante el suministro de potencia activa adicional por parte del controlador de estatismo.

El modelo Simulink del aerogenerador se muestra en la [Figura 2](#). Tiene en cuenta la [Ecuación 1](#) para obtener la potencia mecánica a partir de la velocidad medida del rotor. Utiliza la curva deloaded de la [Ecuación 1](#) para establecer la potencia de referencia. La curva MPPT de la misma figura se utiliza para conocer la saturación del punto de estatismo sumado a la potencia de referencia  $P_{ref*}$ . Esta potencia de salida, al pasar por el convertidor del lado de la máquina, se convierte en la potencia eléctrica real que suministra el aerogenerador.

A continuación, los aerogeneradores pueden integrarse en el sistema eléctrico poniéndolos en paralelo y conectando los unos a los otros en función de la penetración de energía eólica deseada.

La frecuencia en estado estacionario y la carga deslastrada por el mecanismo UFLS pueden obtenerse simplemente tomando el último elemento de cada vector de salida que se obtiene de la simulación. Por otro lado, la frecuencia nadir se obtiene buscando el valor mínimo en estos mismos vectores con valores de frecuencia.

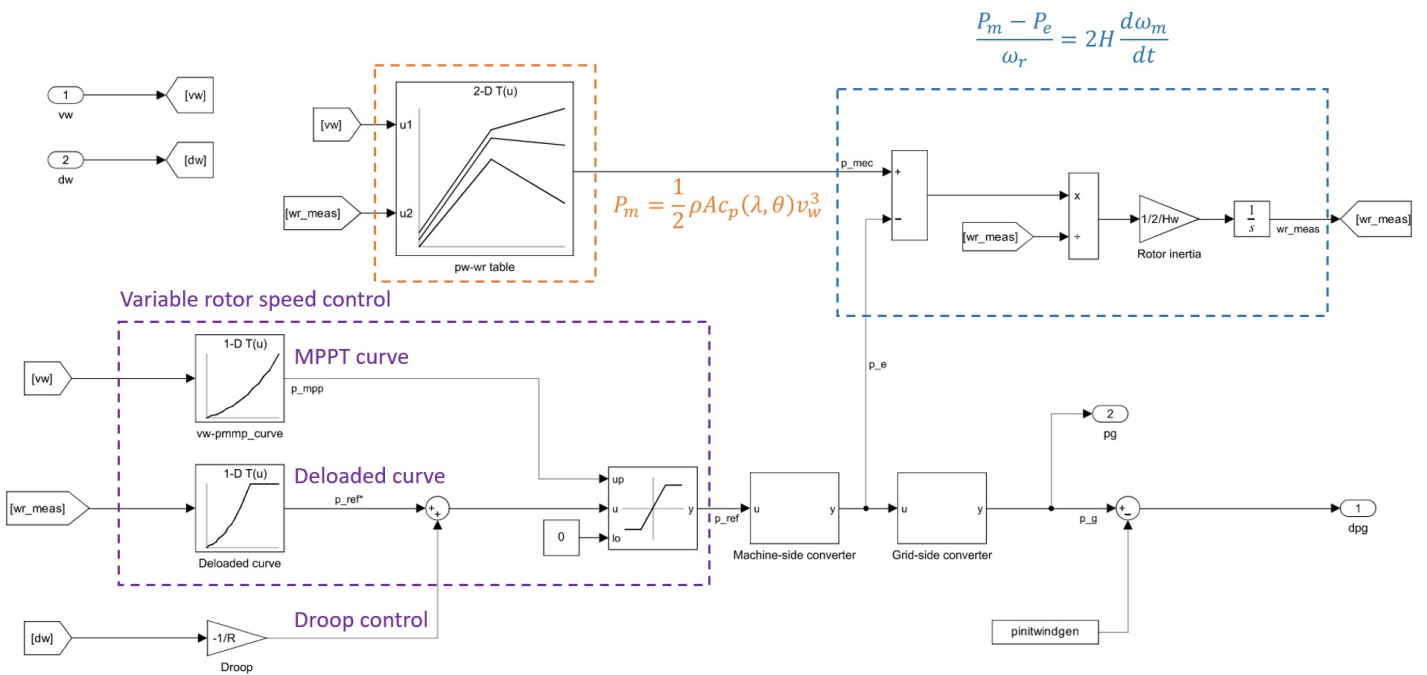


Figura 2: Modelo del aerogenerador en Simulink.

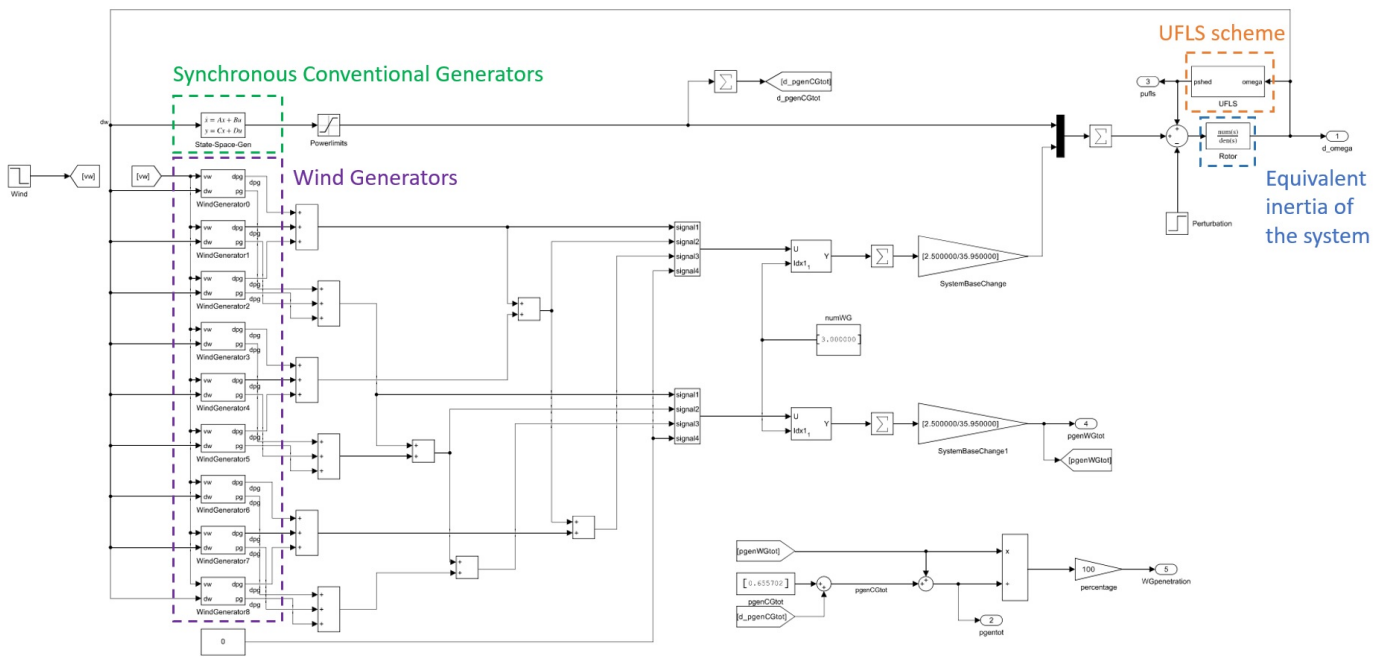


Figura 3: Modelo del sistema de potencia en Simulink.

## Resultados

Es posible cuantificar el impacto del número de GEs, las variaciones de la velocidad del viento y el momento en que se producen estos cambios. Una forma de evaluarlo

consiste en sumar, respectivamente, la carga deslastrada total y la desviación de frecuencia máxima en todas las simulaciones, centrándose en cada parámetro específico. Los resultados se presentan en [Tabla 1](#), [Tabla 2](#), y [Tabla 3](#).

Se puede observar que a medida que la penetración de los GEs es mayor, tanto la desviación de la frecuencia nominal como la carga delastrada son mayores. Esto demuestra que, en general, cuando se conectan más GEs al sistema, éste se vuelve menos estable. De [Tabla 2](#) se deduce que, a medida que aumenta la variación de la velocidad del viento, también aumenta la inestabilidad del sistema. No obstante, [Tabla 3](#) muestra que el momento en que se produce el cambio de viento no es tan significativo, sin embargo su impacto es mayor cuando el viento cambia al mismo tiempo que el evento de frecuencia.

Tabla 1: Suma de la potencia deslastrada y de las desviaciones máximas de la frecuencia base de todas las simulaciones, en función del número de GEs en el sistema.

	3 GEs	6 GEs	9 GEs
$\Sigma P_{ufls}$	2172.1	2408.2	2617.5
$\Sigma \Delta f_{min}$	1450.4	1468.4	1504.7

Tabla 2: Sumas de la potencia deslastrada y las desviaciones máximas de la frecuencia base de todas las simulaciones, en función del cambio de velocidad del viento.

	0 m/s	0.5 m/s	1 m/s
$\Sigma P_{ufls}$	2084.5	2327.5	2785.8
$\Sigma \Delta f_{min}$	1338.9	1479.9	1604.6

Tabla 3: Sumas de la potencia deslastrada y las desviaciones máximas de la frecuencia base de todas las simulaciones, en función del momento del cambio de velocidad del viento.

	-2 s	0 s	+2 s
$\Sigma P_{ufls}$	2381.8	2470.8	2345.2
$\Sigma \Delta f_{min}$	1486.6	1502.0	1434.8

## Conclusiones

Al analizar los totales acumulados de la demanda deslastrada y de la desviación de la frecuencia en todas las simulaciones imaginables, surge un patrón claro. A medida que aumenta el número de GEs integrados, el sistema experimenta una mayor inestabilidad. Del mismo modo, a medida que aumenta el cambio de velocidad del viento, el sistema se vuelve cada vez más inestable. Además, el momento preciso de la caída de la velocidad del viento resulta ser menos influyente en comparación con otros parámetros. No obstante, se alcanza un nivel más crítico cuando la velocidad del viento cae simultáneamente con un evento de frecuencia.

La acción de control implementada en este proyecto reacciona únicamente a los cambios en la velocidad del viento y la desviación de la frecuencia. Sería muy valioso introducir un mecanismo de control destinado a aumentar la potencia durante las inevitables reducciones. En los casos en los que se produce un evento de frecuencia mientras se opera en el modo deloaded con una velocidad del viento constante, la velocidad del rotor se desacelera. Sin embargo, siguiendo el modo deloaded, la potencia disminuye

---

de forma natural.

Este proyecto presenta oportunidades de mejora en varios aspectos. La modelización del aerogenerador podría mejorarse incluyendo un control de ángulo de paso o un control de parada. El uso de un modelo discretizado con una frecuencia de muestreo y la adición de ruido podrían hacer más realista el control de velocidad variable del rotor. La modelización del viento podría mejorarse si se tuvieran en cuenta más parametrizaciones entre los distintos aerogeneradores y los distintos patrones de viento. Investigar la tasa de cambio de frecuencia y tener en cuenta indicadores adicionales de estabilidad de la red podría ser beneficioso para una visión más profunda y holística.



# Bibliografía

- [1] P. Kundur et al. “Definition and classification of power system stability IEEE/CIGRE joint task force on stability terms and definitions”. En: *IEEE Transactions on Power Systems* 19.3 (2004), págs. 1387-1401. doi: [10.1109/TPWRS.2004.825981](https://doi.org/10.1109/TPWRS.2004.825981).
- [2] L. Sigríst, E. Lobato, F.M. Echavarren, I. Egido y L. Rouco. *Island Power Systems*. CRC Press, Taylor & Francis Group, 2016. isbn: 9781498746380.
- [3] IRENA. *Renewable Capacity Statistics 2022*. Último acceso: 29-06-2023. IRENA, 2022, pág. 14. isbn: 978-92-9260-428-8. url: <https://www.irena.org/publications/2022/Apr/Renewable-Capacity-Statistics-2022>.
- [4] O. Apata y D.T.O. Oyedokun. “An overview of control techniques for wind turbine systems”. En: *Scientific African* 10 (2020), e00566. issn: 2468-2276. doi: <https://doi.org/10.1016/j.sciaf.2020.e00566>. url: <https://www.sciencedirect.com/science/article/pii/S2468227620303045>.
- [5] J.G. Slootweg, S.W.H. de Haan, H. Polinder y W.L. Kling. “General model for representing variable speed wind turbines in power system dynamics simulations”. En: *IEEE Transactions on Power Systems* 18.1 (2003), págs. 144-151. doi: [10.1109/TPWRS.2002.807113](https://doi.org/10.1109/TPWRS.2002.807113).
- [6] Kara Clark, Nicholas W. Miller y Juan J. Sanchez-Gasca. *Modeling of GE Wind Turbine-Generators for Grid Studies*. Inf. téc. Version 4.5. One River Road, Schenectady, NY 12345, USA: General Electric International, Inc., abr. de 2010. url: [https://www.researchgate.net/publication/267218696\\_Modeling\\_of\\_GE\\_Wind\\_Turbine-Generators\\_for\\_Grid\\_Studies\\_Prepared\\_by](https://www.researchgate.net/publication/267218696_Modeling_of_GE_Wind_Turbine-Generators_for_Grid_Studies_Prepared_by).
- [7] James F. Conroy y Rick Watson. “Frequency Response Capability of Full Converter Wind Turbine Generators in Comparison to Conventional Generation”. En: *IEEE Transactions on Power Systems* 23.2 (2008), págs. 649-656. doi: [10.1109/TPWRS.2008.920197](https://doi.org/10.1109/TPWRS.2008.920197).
- [8] Hongtao ma y Badrul Chowdhury. “Working towards frequency regulation with wind plants: Combined control approaches”. En: *Renewable Power Generation, IET* 4 (ago. de 2010), págs. 308-316. doi: [10.1049/iet-rpg.2009.0100](https://doi.org/10.1049/iet-rpg.2009.0100).

# Contents

<b>1 Introduction</b>	<b>3</b>
1.1 Context	3
1.2 Purpose of the project	4
1.3 Approach	4
1.4 Alignment with the United Nations Sustainable Development Goals	5
<b>2 State of the art</b>	<b>7</b>
2.1 Modelling of the wind generator	7
2.1.1 Mechanical wind power	7
2.1.2 Control	8
2.2 Modelling of the power system	8
<b>3 Developed Model</b>	<b>11</b>
3.1 Objectives and specifications	11
3.2 Data	12
3.3 Implementation	12
3.3.1 Wind generator model	12
3.3.2 Power system model	16
3.3.3 Storing and visualisation	18
3.4 Cost of implementation	20
<b>4 Analysis of results</b>	<b>21</b>
4.1 Base case	21
4.1.1 Scenarios	21
4.1.2 Generator lost	23
4.1.3 Effect of the droop control	23
4.2 Sensitivity analysis	25
4.2.1 Wind generator penetration	25
4.2.2 Wind speed change	28
4.2.3 Timing of the wind change	28
4.2.4 Sensitivity analysis on all simulations	31
<b>5 Conclusions</b>	<b>33</b>
5.1 Conclusions on the methodology	33
5.2 Conclusions on the results	33
5.3 Recommendations for future research	34
<b>6 Appendix</b>	<b>37</b>
6.1 Data and specifications	37
6.2 Code	39
6.2.1 Main file	39
6.2.2 Power-speed curve	45
6.2.3 Setting Simulink parameters	47
6.2.4 Plotting and printing data	49

6.2.5	Obtaining the sum of the frequency deviations and load shed of all simulations for the each parameter . . . . .	51
<b>Bibliography</b>		<b>55</b>

# Chapter 1

## Introduction

### 1.1 Context

Ensuring frequency stability in a power system is of paramount importance. It is the cornerstone that determines the system's ability to establish and maintain equilibrium between generation and load, while minimizing unintended loss of load [1]. When the frequency drops below a specific threshold, load disconnection through Under-Frequency Load Shedding (UFLS) schemes becomes necessary. Essentially, this situation leads to a partial blackout, highlighting the criticality of frequency stability. The stability hinges upon the combined inertia of rotating masses in prime movers and generators, along with the primary frequency regulation provided by the prime movers in the system [2]. In the context of island power systems, which are small and isolated, susceptibility to active power disturbances is heightened. Due to the limited number of available generators, the overall inertia and primary frequency regulation capacity remain comparatively low in comparison to interconnected power systems.

Meanwhile, the world is experiencing a change in its energy generation mix. The renewable energy sector has seen an increasing penetration in the energy market, particularly wind power [3]. Notably, the European Union (EU) has nearly doubled its wind energy capacity from 2012 to 2021 [3]. This substantial growth has led to a gradual replacement of conventional generators (CGs) with wind generators (WGs). However, the higher penetration of WGs introduces challenges for frequency stability in the power system. Most renewable energy sources, including WGs, are connected to the grid through power converters, which mechanically decouple them from the system. Consequently, WGs exhibit no rotating inertia to the system unless it is emulated through power electronics schemes. This lack of inherent inertia contributes to a reduction in the system's frequency stability. Furthermore, wind turbines (WTs) typically operate in Maximum Power Point Tracking (MPPT) mode, where they continuously extract the maximum possible power from the wind. Unlike synchronous generators, this operating mode does not prioritize providing primary frequency regulation to the grid. As a result, the increased penetration of WGs, operating in MPPT mode and lacking inherent inertia, further strains the system's frequency stability.

This loss in rotating inertia and primary frequency regulation capacity due to the increasing penetration of renewable energy sources further challenges frequency stability of island power systems. Their small scale results in a low inertia, so that, if a generator trips, the initial Rate of Change of Frequency (ROCOF) is greater than in larger and more interconnected systems. Consequently the minimum frequency reached is lower (the steady-state frequency remains the same). This makes it more likely for the UFLS scheme to be activated, resulting in the disconnection of load. Nonetheless, frequency stability can also be improved by requiring WGs to provide primary frequency regulation. WGs can technically offer primary reserve in order to carry out primary frequency regulation. WGs can be configured to operate in a deloaded mode, enabling them to supply additional power to the grid when necessary. This deloaded operation is achieved by deliberately adjusting the rotor speed of the turbines. Advancements in control strategies and grid integration techniques have made it possible to enhance the contribution of WGs to primary frequency regulation. Various control mechanisms can enable real-time monitoring and adjustment of WGs' power output to support primary frequency regulation. Primary frequency control provision by WGs does not come without problems though

since the power supplied by WGs is dependent on the wind speed. As wind speed changes, the power output and the availability of primary reserve from WGs also fluctuate. In power systems with a high penetration of WGs, there is a concern that a sudden reduction in wind speed, combined with a trip of a CG, could further accentuate frequency stability. Of course, coordination between WGs and other grid assets, such as energy storage systems, can provide supplementary support to maintain frequency stability during fluctuations in wind power availability, but this may require further investments in new assets.

As the system becomes more reliant on WGs for primary frequency regulation, the effect of a wind speed reduction should be carefully analyzed. The objective of this project is to quantify the change in wind speed that together with a generation tripping would cause UFLS. This information would be helpful to grid operators since the variability and limited predictability of wind speeds poses a problem when planning for power production.

## 1.2 Purpose of the project

It is highly beneficial for a grid operator to quantify the stability of a power system with high wind generator penetration, particularly when a CG is accidentally disconnected during a drop in wind speed. In such situations, the absence of a CG's contribution, combined with reduced wind power output, can lead to frequency deviations and potential instability in the power system.

Quantifying the stability in this scenario allows the grid operator to assess the system's ability to maintain frequency within acceptable limits and avoid a complete system collapse. UFLS schemes may be necessary to address this issue. UFLS schemes are designed to automatically shed a pre-determined amount of load in the event of a significant frequency drop. Since the power generated must always be the same as the power demanded by the grid, shedding load can restore the balance between the two and prevent further frequency deterioration.

Quantifying the stability of the power system under these conditions enables the grid operator to optimize the integration of WGs. It provides insights into the system's resilience, helping in the development of strategies to enhance the power system's ability to withstand sudden changes in generation and load. This knowledge informs decision-making regarding grid expansion, operational planning, and the implementation of appropriate control measures to ensure the reliable operation of the power system.

Additionally, understanding the stability of the power system with high wind generator penetration helps the grid operator to re-adjust the thresholds at which UFLS schemes should be activated. By accurately quantifying stability, the operator can determine the level of load shedding required and its activation mechanism to maintain frequency stability during contingencies, such as the accidental disconnection of a CG combined with a drop in wind speed. This proactive approach mitigates the risk of widespread blackouts and minimizes the impact on customers.

Overall, the ability to quantify the stability of a power system with high WG penetration during contingencies involving the accidental disconnection of CGs and drops in wind speed is essential for effective system management. It allows the grid operator to activate appropriate UFLS schemes, optimize WG integration, and maintain the stability and reliability of the power system for the benefit of consumers and the grid as a whole.

## 1.3 Approach

To achieve the purpose of the project, three tasks will be carried out:

- Modelling of the WG
- Integration of the WG into the System Frequency Dynamics (SFD) model of the power system
- Analysis of the simulation outputs defining the frequency stability of the power system

The study approach of this project will be based on time-domain simulations using MATLAB code integrated with Simulink models to accurately represent the frequency response of a power system incorporating WGs. Time-domain simulations provide a detailed and dynamic analysis of system behavior, allowing for the examination of transient responses and the evaluation of system stability. An analytical approach would be impractical and overly simplified due to the non-linear nature of the WG and power system model. By leveraging the computational power of MATLAB and the flexibility of Simulink, the project can capture the complex interactions between the power system components, including the WGs.

The simulations will be conducted for various scenarios, considering different parameters such as wind speed, turbine characteristics, and system load variations. The frequency response obtained from these simulations will be stored and plotted to analyze the dynamic behavior of the power system under different conditions. This will provide valuable insights into the system's response to frequency deviations caused by WG integration.

Furthermore, the project will perform a sensitivity analysis to explore the impact of parameter variations on the frequency response. Sensitivity analysis helps in identifying critical parameters that significantly influence system behavior, allowing for better understanding and optimization of the power system with WGs.

## 1.4 Alignment with the United Nations Sustainable Development Goals

This project aligns with several of the United Nations (UN)' Sustainable Development Goals (SDGs), however it predominantly addresses the SDG 7, “*Ensure access to affordable, reliable, sustainable and modern energy for all*” [4]. The target 7.1 is of particular importance:

*Target 7.1: By 2030, ensure universal access to affordable, reliable and modern energy services*

While it may not directly ensure in the short-term that more people have access to electricity (indicator 7.1.1), it is crucial in the long-term so that people have access to clean fuels and technology (indicator 7.1.2). Understanding how the system frequency is affected when the loss of a generator coincides with a drop in wind speed is crucial for ensuring reliable and resilient energy services. By assessing the potential instabilities that may arise in such situations, this project pretends to contribute to the reliable operation of power systems, which is essential for providing uninterrupted energy services to consumers. Even though the reliability of the grid is directly mentioned in this target, it is not directly specified through an indicator. Nonetheless, this project does quantify it through the measurement of the shedded load in the power system under study. This knowledge can inform policymakers, energy planners, and operators in making informed decisions regarding the deployment, grid integration, and optimization of wind energy resources, ultimately facilitating the goal of universal access to affordable, reliable, and modern energy services.

*Target 7.2: By 2030, increase substantially the share of renewable energy in the global energy mix*

This project aligns with target 7.2 since it admits that in order to have a high share of renewables in the power system, frequency regulation schemes are of great importance. The concept of WGs being able to provide primary frequency stability, even if it is not a stand-alone solution to target 7.2, is useful to grid operators. The indicator of this target will be quantified in this project through the WG penetration.

*Target 7.b: By 2030, expand infrastructure and upgrade technology for supplying modern and sustainable energy services for all in developing countries, in particular least developed countries, small island developing States, and land-locked developing countries, in accordance with their respective programmes of support*

This target is particularly relevant for small island and land-locked regions that often face unique challenges in maintaining reliable energy systems due to limited inertia. The findings of this research can help guide the upgrading of infrastructure and the adoption of advanced technologies in these regions. This project intends to improve the indicator 7.b.1. It quantifies the installed renewable energy-generating capacity in developing countries (in watts per capita). In this project this is simulated and explored through WG penetration.

# Chapter 2

## State of the art

This section intends to provide an overview of the existing knowledge, research, and advancements related to WG modelling and power system modelling in the context of high WG penetrations. It delves into the current state of the field, examining the key concepts, methodologies, and challenges associated with accurately representing WGs and power systems in simulation models. This section encompasses a review of relevant literature, research studies, and technological developments that have contributed to the understanding of WG modelling techniques, power system dynamics, and the interaction between the two. By exploring the state of the art in WG and power system modelling, this section establishes a foundation for the subsequent analyses and findings of this project.

### 2.1 Modelling of the wind generator

This section explores the dynamics and control aspects of WGs. WGs play a crucial role in renewable energy systems by harnessing the power of wind to generate electricity. Understanding the dynamics of WGs and the control mechanisms employed is essential for effectively integrating them into power systems. An overview of the current state of knowledge regarding WG modeling is carried out here, including the key considerations in capturing their dynamic behavior and the various control strategies employed to optimize their performance.

There are two main types of WGs that allow the rotor to vary its rotational speed [5]. The first, the Doubly-Fed Induction Generator (DFIG)-based wind turbine, works with a variable speed wind turbine with a partial power converter or a wind turbine with, as its name suggests, a DFIG. The second is the Full Converter Variable Speed Wind Turbine (FCWT). This one can make use of different generators such as induction or synchronous ones, with either permanent magnets or external electrical excitation.

#### 2.1.1 Mechanical wind power

An important equation is shown in Equation 2.1. It quantifies the mechanical power of a WG. It is a simplified model that is often used to assess their performance [6, 7, 8].

$$P_m = \frac{1}{2} \rho A_w c_p(\lambda, \theta) v_w^3 \quad (2.1)$$

$P_m$  is the mechanical power (in  $W$ ),  $\rho$  is the air density (in  $kg/m^3$ ),  $A_w$  is the area swept by the blades (in  $m^2$ ),  $c_p$  is the performance coefficient,  $v_w$  is the wind speed (in  $m/s$ ) and  $\lambda$  is the tip speed ratio:

$$\lambda = \frac{\omega_r R}{v_w} \quad (2.2)$$

defined by the the radius of the blades  $R$  and the rotor speed  $\omega_r$ . Depending on the literature, it may also be written in terms of mechanical torque rather than mechanical power [9]:

$$T_m = \frac{1}{2} \rho A_w c_p(\lambda, \theta) R v_w^2 \quad (2.3)$$



The performance coefficient is simply a convenient way to numerically approximate the mechanical power or torque of the WG. This is one of the reasons why its values may vary in the current literature. Evidently, these values also depend on the specific model of the turbine. The paper in [6] proposes a mechanical model with a  $c_p$  characteristic that applies to WG that have a nominal power ranging from 750 kW to 2.5 MW. This paper specifically indicates what values has to be given to the radius  $R$  depending on the nominal power chosen. Additionally, the minimum and the nominal rotor speeds have to be met accordingly.

This simplified model is employed to provide a quick and practical estimation of the wind turbine's electrical behavior within a power system. By considering key variables such as air density, rotor swept area, power coefficient, and wind speed, the model allows for a straightforward evaluation of the wind turbine's power output. Although it may not capture all the intricacies of the turbine's performance, this approach is valuable in assessing the overall electrical behavior of the system and making informed decisions regarding its integration and operation within the power grid.

This modelling also simplifies the wind speed as a parameter of the system. Rather than using an array of wind speed signals that impact onto the blades of the rotor, a single wind speed signal is used to better analyse its impact on the frequency response.

### 2.1.2 Control

WGs need controls in order to effectively offer primary frequency regulation in power systems. WGs may actively monitor and react to frequency variances by putting advanced control procedures into practice, which helps to stabilize system frequency. Based on the frequency changes, these control mechanisms enable WGs to modify their power output, optimize rotor speed, and fine-tune blade pitch angles. WGs can support primary frequency management by precise control measures, improving the overall stability and dependability of power networks with greater wind energy integration.

In the case of DFIG and FCWT WGs, the rotor's rotational speed can be controlled so as to adjust the electric power produced in reaction to frequency variations. It is considered to be one of the most efficient and reliable controller [10]. It is the most common controller applied alongside the pitch angle controller. On the other hand, there is also the pitch angle controller. It is comparatively slower than the rotor speed one, with the blades' pitch angle moving at a typical rate of  $2^\circ/s$  [11] and at most  $10^\circ/s$  [6] depending on the size of the wind turbine. However, it can be beneficially used to avoid mechanical damage and ensure safe operation of the WG's blades at higher wind speeds [12, 10]. The rotor speed control and the pitch angle control can be combined as shown in [11] and [13].

Among the different options to activate primary frequency control, droop control has been commonly proposed. The droop control provides an additional input signal to the aforementioned rotor speed and pitch angle controllers. Whereas deloading controller acting for instance on the rotor speed provides for the necessary headroom (power margin), the droop control activates this power margin and ensures that it is injected into the grid. The most typical configuration is to provide a droop power directly proportional to the frequency deviation, however other studies suggest the use of a variable droop [14]. It is intended to smoothen power fluctuations and contribute more to primary frequency regulation.

In extreme weather conditions in which the wind speed may be so large that it may tear the turbine apart, stall power control can come into play [10]. Its two ramifications, passive and active stall power control, activate the WG's brakes when it reaches a cut-out speed. The passive version is simpler in the sense that when this threshold is reached, the blades are bolted to the hub at a fixed angle. It requires less control efforts and the installation of additional actuators. Meanwhile active stalling activates similarly to pitch angle control. Nonetheless, unlike pitch angle control, it cannot keep a constant power output, and it turns the turbine blades into the wind rather than away in order to reduce the lift force on the blades.

## 2.2 Modelling of the power system

The power system model used in this project is based on a SFD model [2] due to its simplicity in capturing the dynamic behavior of the power system, particularly in relation to frequency deviations. It represents the interconnected generators, loads, and transmission network as a simplified, aggregated

system where the frequency is assumed to be uniform (in reality, frequency is only uniform in steady state, whereas frequencies differ throughout the power system in transient state). By considering the system as a whole, rather than its constituent components, the SFD provides a holistic view of the system's response to disturbances and changes in power generation. This approach facilitates the evaluation of the impact of WGs on system stability. Additionally, the SFD is widely used in research and industry, providing a well-established framework for analyzing and designing control strategies for power systems with renewable energy sources like WGs. Therefore, by utilizing the SFD in the time-domain MATLAB/Simulink simulation, this project can effectively assess the frequency deviation dynamics and evaluate the performance of the power system with WGs.

In the SFD model, CGs are represented by a generic second-order system. This in turn can be described by a state space and a saturation in series in [2]:

$$\begin{bmatrix} \Delta \dot{x}_{1tg} \\ \Delta \dot{x}_{2tg} \end{bmatrix} = \begin{bmatrix} 0 & 1 \\ \frac{-1}{a_{1,i}} & \frac{-a_{1,i}}{-a_{2,i}} \end{bmatrix} \begin{bmatrix} \Delta x_{1tg,i} \\ \Delta x_{2tg,i} \end{bmatrix} + K_i \begin{bmatrix} 0 \\ \frac{1}{a_{2,i}} \end{bmatrix} \Delta \omega \quad (2.4)$$

$$\Delta p'_{G,i} = \left[ 1 - \frac{b_{2,i}}{a_{2,i}} \quad b_{1,i} - \frac{a_{1,i} \cdot b_{2,i}}{a_{2,i}} \right] + K_i \cdot \frac{b_{2,i}}{a_{2,i}} \Delta \omega \quad (2.5)$$

Where  $a_{1,i}$  and  $a_{2,i}$  are the poles and  $b_{1,i}$  and  $b_{2,i}$  are the zeroes of the generic second-order system,  $K_i$  is the inverse of the droop in pu in the power rating base of the generator. The saturation of the generated power  $\Delta p'_{G,i}$  between a minimum and a maximum power output converts this linear system into a non-linear one, already making a time-domain simulation necessary rather than a purely analytical analysis.

The WGs may be integrated into the power system by adding their outputs in parallel and make the necessary base change adjustments as shown in [12] and [14]. It is not converted into a state-space due to its non-linear nature as seen from the equation of motion represented in Equation 2.1.



# Chapter 3

## Developed Model

### 3.1 Objectives and specifications

The main objective of this model is to be able to evaluate the frequency response of the grid under a variety of different conditions, or parameters:

1. *Time of the day*: 24 scenarios with different CGs providing different active power configurations have been considered. Each scenario represents one hour of the day. As time passes by, some of the CGs get connected, disconnected or change their power contribution.
2. *Generator being shut down*: there may be a different amount of generators connected at each scenario, each possibly generating a different amount of power. This means that which generator gets disconnected could significantly impact the frequency response.
3. *Number of WGs in the system*: a greater number of WGs in the system would mean that, if a CG gets disconnected, the primary frequency regulation of the WGs would be able to compensate for that loss in power, thus providing more stability. On the other hand, if the grid has a high WG penetration, a sudden drop in wind speed will decrease the power generated, thus decreasing the stability.
4. *Wind speed change*: as the wind speed change becomes more drastic, so does the frequency response of the system. The WGs would drop their power contribution more significantly, thus reducing the stability of the system.
5. *Time at which the wind speed changes*: the wind speed may change before, after or during the disconnection of the CG. The timing at which this drop in wind speed occurs may also affect the stability of the system. For example, if the drop in wind speed occurs at the same time as the generator incident, it can be said with complete certainty that the ROCOF would be of greater magnitude.

The possible parameters values are shown in [Table 3.1](#).

Once the model is described, a MATLAB script will coordinate the setting of all parameters according to the fixed specifications of all components and the aforementioned parameters. The script

Parameter	Values
Time of the day	1, 2, ... 24
Generator number being shut down	11, 12, ... 21
WGs connected	3 6 9
Wind speed change (m/s)	0 0.5 1
Time at which the wind speed changes, in respect to the time of incident (s)	-2 0 2

Table 3.1: Parameter values.

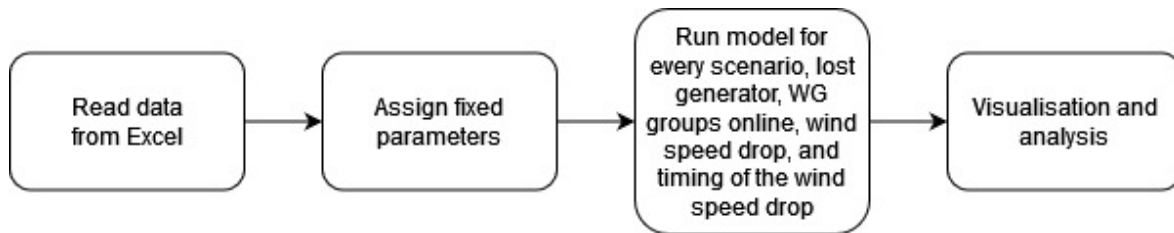


Figure 3.1: Flowchart of the MATLAB script.

will run the Simulink model and record several outputs in the time domain. This data can then be visualised and analysed. Figure 3.1 shows the flow of tasks carried out by the script.

For the purpose of comparing the effects of each of these parameters on the system, three values are measured: the minimum frequency reached, the steady-state frequency and the power shed by the UFLS scheme. These give a quantitative evaluation of the configuration performing the provision of stability.

## 3.2 Data

The data handled in this project (provided by the supervisor) comes from the Spanish island of La Palma in the Canary Islands. The data specifies the generator and the UFLS scheme specifications, as well as the active power generated by the multiple CGs throughout the day, in 1 hour intervals.

The CGs have an associated inertia, a base apparent power, a maximum and minimum power ratings, and four values that are used to determine the state-space model representing the set of CGs that are not going to be disconnected during the simulation. This data can be seen in ?? of the appendix. On the other hand, the WGs used in this project have a nominal power rating of 1.5 MW with a diameter of 65 meters.

The specifications of the UFLS scheme are also specified, as shown in Table 6.1 in the appendix. Each substation or bus has a particular set of parameters. The UFLS scheme detaches a load at a particular substation when a certain frequency or ROCOF crosses a threshold for a specified amount of time (i.e. an intentional delay). This deloading takes a few milliseconds to take place (i.e. an opening delay). In this project, the threshold frequency is set in a range between 47 and 49.5 Hertz. This has the intention to comply with the Spanish technical regulations on isolated power systems. These regulations state that the UFLS schemes must prevent the frequency from falling below 47.5 Hertz for more than 3 seconds [15].

Finally, the generation scenarios show how much active power the CGs connected to the buses with identification numbers from 11 to 21 generate within a 24-hour day. This data is shown in Table 6.1. It can be deduced early on that the most noticeable changes in frequency will be seen when disconnecting generators 17 and 21, since these produce the most active power compared to the other ones. The last column shows the power generated by a single, 1.5 MW WG.

## 3.3 Implementation

This section describes the developed models and their implementation. The implementation of the final power system model involves several components. These include the state-space model of the CGs, the connection of the multiple WGs, the UFLS scheme and the inertia of the system. The first two represent the “generation side” of the system while the two latter components represent the system itself (a uniform frequency can be coined as a system frequency and UFLS is a system-wide protection).

### 3.3.1 Wind generator model

Wind turbines extract wind energy by capturing the wind’s force with their rotor blades, causing them to rotate. This rotational energy is then converted into mechanical power by a gearbox connected

to a generator. The generator transforms this mechanical power into electrical energy, which can be then be directed towards the power system. A control is needed in order to set the adequate electrical power that is meant to be more convenient for the power system operators.

A WG model may take the wind speed and the frequency deviation of the power system as inputs to accurately determine its operational behavior and optimize its performance. The wind speed provides crucial information about the available kinetic energy in the wind, which directly affects the power output of the turbine. By incorporating wind speed data into the model, it can adjust its blade pitch angle, rotational speed, and other parameters to harness the maximum energy from the wind.

Additionally, the frequency deviation of the power system serves as an essential indicator of the grid's stability and demand-supply balance. The WG needs to adapt its output to match the grid's requirements, especially during transient conditions or frequency deviations caused by sudden load changes or disturbances. By monitoring the frequency deviation, the WG model can respond promptly by adjusting its power output or employing advanced control strategies to support grid stability.

Therefore, by considering both the wind speed and the frequency deviation of the power system, the WG model can optimize its performance, maximize energy extraction, and contribute to a reliable and stable electrical grid.

The power generated by the WG and its deviation from its initially generated power are used to fit into the existing power system model that primarily considers frequency deviations. While wind speed provides valuable information for optimizing the performance of the WG, the power system model focuses more on the overall grid stability and maintaining a balanced power supply. By integrating the power generated by the WG and its deviations into the existing model, system operators can accurately monitor the power injection from the wind farm and assess its impact on the grid's frequency deviations. This information is crucial for grid operators to make informed decisions and take appropriate control actions to ensure the stability and reliability of the entire power system. By incorporating power generation data into the model, it enables a comprehensive analysis of the WG's contribution to the grid and facilitates efficient power system management.

## Rotor

Wind turbines extract wind energy and convert it into mechanical power through a series of complex mechanisms involving aerodynamics. The process begins with the wind's kinetic energy, which is harnessed as it flows through the turbine's rotor blades. These blades are designed to capture as much wind energy as possible, utilizing their large surface area and aerodynamic shape. As the wind strikes the blades, it exerts a force on them, causing them to rotate. This rotation is then transferred to the main shaft of the turbine, which is connected to a gearbox, increasing the rotational speed. The gearbox drives a generator, which converts the mechanical power into electrical energy.

When evaluating the mechanical behavior of a power system, a simplified model is often used to assess the performance of wind turbines [6]. This model has been already presented in Equation 2.1 in subsection 2.1.1.

Of course, this mechanical power can be divided by the nominal power of the WG ( $P_n$ ) in order to switch to *pu* units. The performance or power coefficient is itself dependent on the pitch angle of the blades  $\theta$  (in degrees) and the tip speed ratio  $\lambda$ . This performance coefficient can be numerically approximated with Equation 3.1 [16]:

$$c_p(\lambda, \theta) = 0.73 \left( \frac{151}{\lambda_i} - 0.58\theta - 0.002\theta^{2.14} - 13.2 \right) e^{-18.4/\lambda_i} \quad (3.1)$$

where

$$\lambda_i = \frac{1}{\frac{1}{\lambda - 0.02\theta} - \frac{0.003}{\theta^3 + 1}} \quad (3.2)$$

This simplified approach to modelling saves development time since there is not as much need to obtain detailed information about the rotor's geometry from the manufacturers. However, most importantly, it also saves a significant amount of computation time, as not only does it avoid the need for more specialised fluid-mechanics software, but also Equation 2.1 can be predefined onto a look-up table.

This relationship between the mechanical power  $P_m$ , the rotor speed  $\omega_r$  and the wind speed  $v_w$  can not only be predefined onto a look-up table, but also plotted, as shown in Figure 3.2.

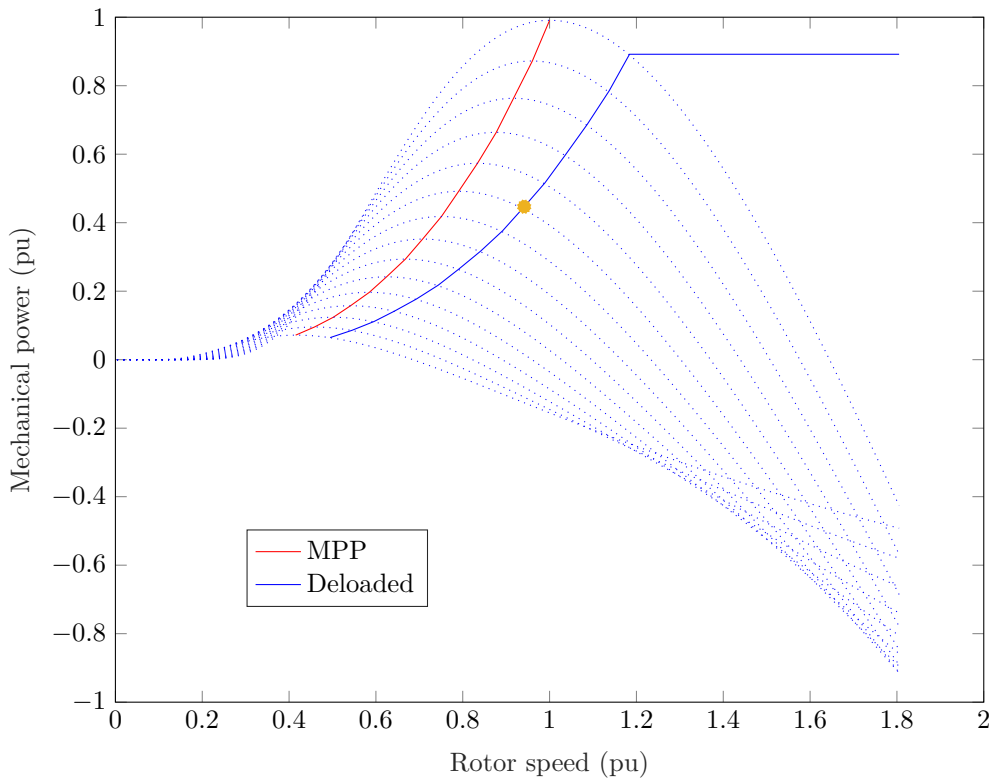


Figure 3.2: Power-speed plot at a  $0^\circ$  pitch angle. The wind speeds range from 5 to 12  $m/s$ , in 0.5  $m/s$  intervals. The WGs are initialised in any equilibrium position along the deloaded curve. An example of a starting operating point is shown in orange.

### MPPT and deloaded operation

While a certain mechanical power is generated from the rotor, it is desired to set a particular power for the purpose of providing primary frequency control. This can be achieved through the creation of a primary reserve, that is, initially generate less active power than the maximum possible so that, in the unfortunate case of a drop in the system frequency, the WG can provide more power and smoothen out the transient and decrease the change in the steady-state.

Given a particular wind speed, the WG can provide only a certain amount of mechanical power. The purpose of using a MPPT scheme is to always establish those operation points as a setpoint, no matter what the wind speed is. A curve can be drawn to represent these points, as shown in [Figure 3.2](#). The curve passes through what are known as the Maximum Power Point (MPP). Under this operation mode, typically a rotor speed control would be in charge of making the WG always provide the maximum quantity of electrical power given the wind speed available. This operation mode makes the most economic sense when there is no need for the frequency stability of the grid, since as more power is generated, more profit is gained.

However this project considers a WG that operates in a deloaded operation mode. The model made for this project has a 10% deloading, meaning that in normal steady-state operating conditions, the WG will miss out on generating 10% of the maximum available power it could provide given its current wind speed. This value for the deloading has simply been chosen because typical values range from 10 to 20% [\[17\]](#); finding the optimal deloading is out of the scope of this project. For these purposes, techno-economic analysis are required as in [\[18\]](#).

The rotor speed is purposefully controlled in order to reach such a deloaded point. In principle, there would be two possible ways to provide 90% of the MPP; decreasing or increasing the rotor speed.

However in practise, the rotor speed is increased, so that only one curve is plotted on [Figure 3.2](#). This is because the decreasing the rotor speed beyond the MPP makes the system unstable [\[19\]](#). [Figure 3.2](#) was made from a MATLAB script that was partially provided by the project supervisor. It was completed by adding the deloaded curve and by programming in such a way that the corresponding wind speed is obtained given a certain generated power and assuming that the WG operates in equilibrium in the deloaded operation mode.

### Generator/converter

The dynamics of the part of the model regarding the integration of its mechanical and electrical parts is based on [\[6\]](#).

$$T_m - T_e = 2H \frac{d\omega_r}{dt} \quad (3.3)$$

Where  $T$  is the torque,  $H$  is the inertia of the rotating mass,  $\omega_r$  is the mechanical frequency at which the rotor rotates and the subindices  $m$  and  $e$  stand for mechanical and electrical, respectively. This differential equation represents the system since, as it can be seen, if the mechanical power decreases to a value below the electrical one, the rate of change in rotor speed becomes negative. For simplicity in the visualisation of the model, this project intends to only deal with powers rather than torques, so that by multiplying  $\omega_r$  on both sides of [Equation 3.3](#), [Equation 3.3](#) can be rewritten as:

$$(T_m - T_e) \cdot \omega_r = P_m - P_e = 2H \frac{d\omega_r}{dt} \cdot \omega_r \quad (3.4)$$

If small variations around the steady-state conditions are considered, it could be possible to remove the  $\omega_m$  term on the left-hand side of [Equation 3.4](#) and obtain [Equation 3.5](#), as outlined in [\[20\]](#). However it was thought that it since this project might deal with extreme situations where load is shed, it would be better to take the rotor speed into consideration.

$$P_m - P_e = 2H \frac{d\omega_r}{dt} \quad (3.5)$$

Essentially, these equations expresses the relationship between power imbalances and the resulting angular acceleration in a rotating mass system. A positive power imbalance indicates that the mechanical power input exceeds the electrical power output, causing the rotor speed to increase. On the other hand, a negative power imbalance suggests that the electrical power output exceeds the mechanical power input, leading to a decrease in rotor speed.

In this model, the mechanical power will come from the look-up table expressing the dynamic behaviour of the rotor (as described by [Equation 2.1](#)), while the electrical power will be the desired electrical power given to the grid. The latter will be subject to a control, as it will now be described.

### Control

The control strategy employed in this project relies purely on rotor speed control. This decision comes from the fact that the project focuses on wind speeds that are in a range that does not need the implementation of pitch angle control. By considering wind speeds that are not extreme, the need for adjusting the pitch angle of the wind turbine blades is thought to be unnecessary.

The rotor speed is regulated with an active power controller [\[13\]](#). It is in charge of controlling the electrical power  $P_e$  provided by the WG. To achieve this goal, it must handle a series of signals:

- Wind speed  $v_w$ : the wind speed determines the maximum power the WG can provide at any point in time (that is, the MPP).
- Measured rotor speed  $\omega_{r_{meas}}$ : the rotor speed determines part of the current electrical power that is provided by the WG.
- Frequency deviation  $\Delta f$ : the WG will provide more power proportional to the severity of the frequency drop.



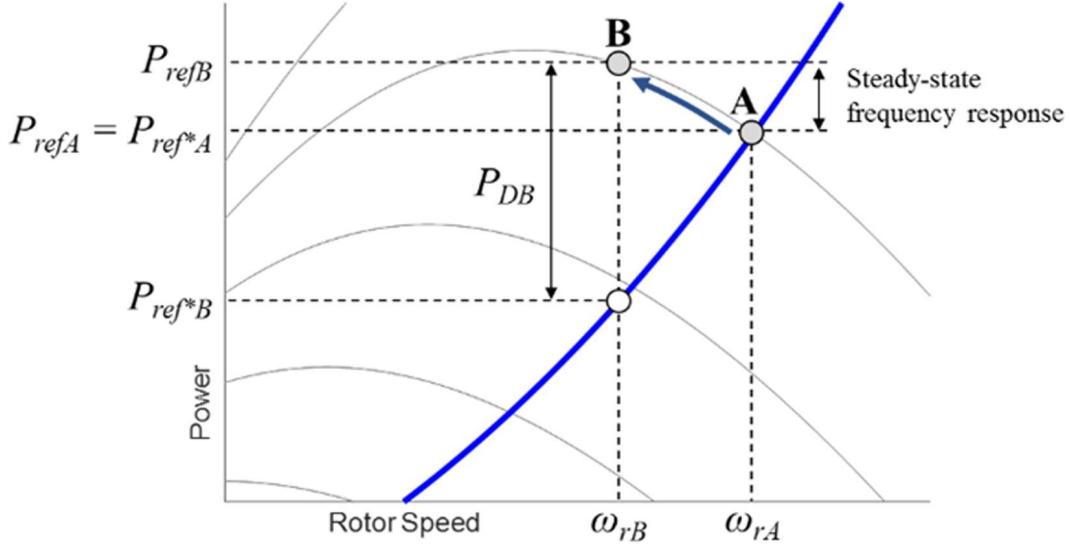


Figure 3.3: Power tracking via power signal feedback. Figure from [13].

The reference signal  $P_{ref}$  intends to represent the desired electrical power outputted. It is essentially the same as the electrical power  $P_e$ , but delayed, since it has not gone through the machine-side converter. This reference signal is obtained by the addition of another reference signal  $P_{ref*}$  with the droop controller. Additionally, the  $P_{ref}$  signal will have to be limited depending on the current wind speed, since that in turn determines the MPP. On Simulink, this is represented with a saturation block with the upper external port connected to a look-up table representing the MPPT curve, while the lower port connected to a “0” constant, since it is assumed that the WG can only generate power.

Furthermore the signal  $P_{ref*}$  is obtained from the tracking characteristic, that is, the deloaded curve. On the Simulink model, this is another look-up table with the deloaded curve. Depending on the current rotor speed, the  $P_{ref*}$  power will change, since the droop power  $P_D$  will add or remove more power depending on the frequency deviation.

Figure 3.3 from [13] shows how such a system would behave. Suppose the system starts in the equilibrium point A, with its respective power  $P_{ref*A}$  and rotor speed  $\omega_{rA}$ . At first, the reference signal  $P_{refA}$  is equal in magnitude as  $P_{ref*A}$  since the system is balanced. Under normal operating conditions, the WG operates following the deloaded curve as the wind speed fluctuates. Nonetheless, when a drop in frequency occurs, the WG must use its primary frequency regulation to provide more power to the grid, perhaps reaching the MPP. Given the wind speed available, the only possible way to do so is by decreasing its rotor speed. The reference  $P_{ref*}$ , that is still following the deloaded curve, decreases. However, a droop power  $P_D$  proportional to the frequency deviation is added onto the reference, thus reaching equilibrium point B.

### Wind generator model

Figure 3.4 shows the WG Simulink model that encompasses all the aforementioned components. The mechanical power provided by the WG (described by Equation 2.1) is described by a look-up table (shown in orange). The control of the electric power, determined by the variable rotor speed control and the droop control, is shown in purple. The relationship between these two variables (described by Equation 3.4) is highlighted in blue.

### 3.3.2 Power system model

Load damping, although an important aspect of power system dynamics, is not explicitly considered in this SFD model [2] due to conservative reasons. The primary purpose of this model is to assess the stability and response of the power system under various operating conditions and disturbances.

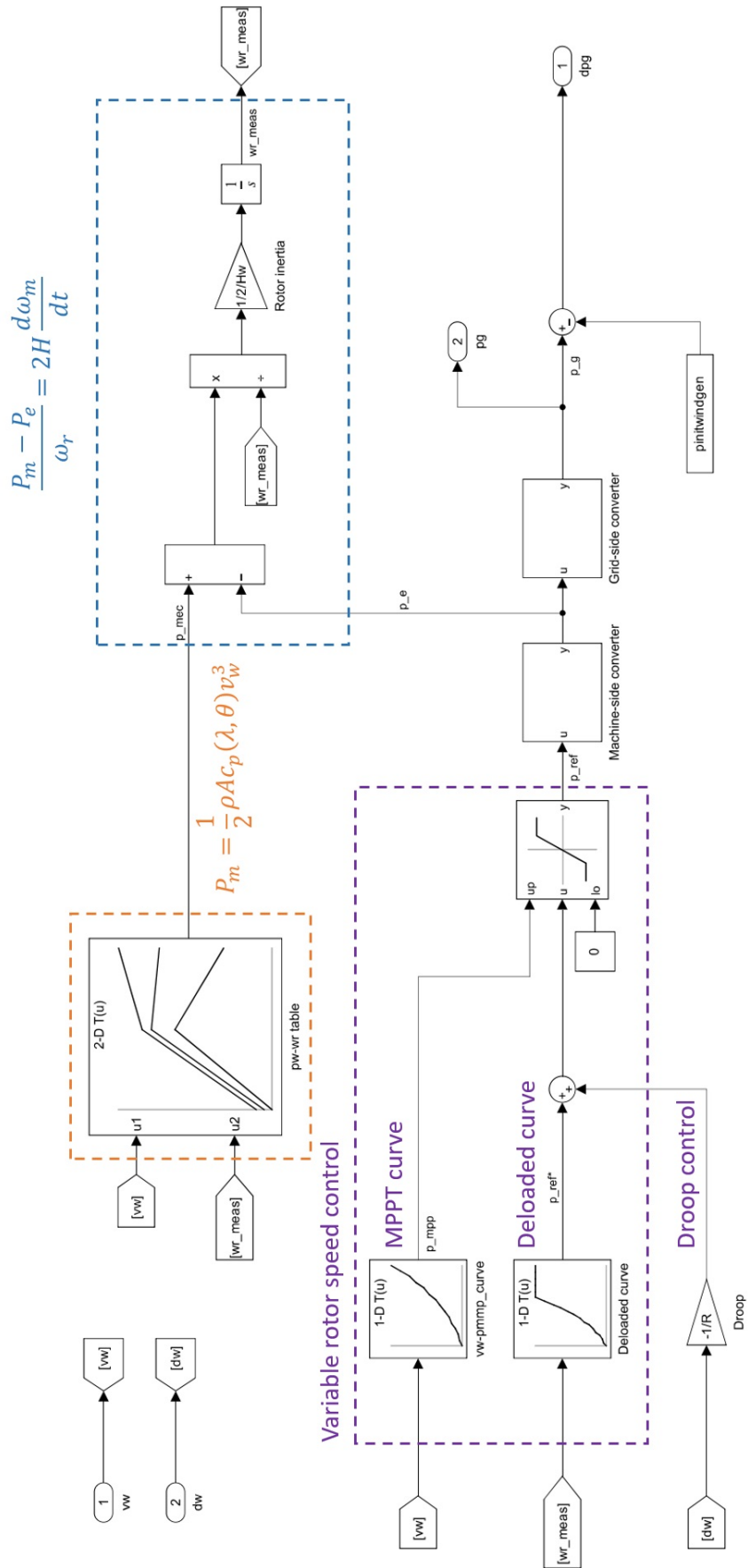


Figure 3.4: Simulink model of the WG.

Due to the complexity and variability of load characteristics, the omission of load damping in the conservative SFD model simplifies the analysis and reduces computational burden. It allows for a more straightforward assessment of the system's stability and response under critical conditions without relying on detailed load modeling assumptions, which can introduce additional uncertainties and potential inaccuracies.

The WGs in the power system have had their respective inputs and outputs connected, as shown in [Figure 3.5](#). The frequency is the same for all components, so a single bus is needed. It has been assumed that the wind speed is the same for all WGs. It is out of the scope of this project to make a more accurate modelling of the wind. However, the WGs have been configured in such a way that if needed, the wind speed may be easily changed and reconfigured for each WG individually.

Since the pre-existing model only treated with deviations, only the deviations in power generated by the WGs fed back into the system. However, a base change is needed from the WG power base defined by the nominal power  $P_N$  to the system base. This system power base  $S_{base}$  is defined on the CGs' base. This is the sum of the rated MVA power of each machine that are not getting shut off.

Nonetheless, the power generated by the WGs is also collected (with its respective base change) so that the Simulink model gets this value and the WG penetration as outputs. This clarifies the behaviour of the WGs in the system in regards to power contribution. The instantaneous WG penetration is calculated within the Simulink file by applying [Equation 3.6](#).

$$WG \text{ penetration} = \frac{P_{gen_{tot}}^{WG}}{P_{dem_{tot}}} = \frac{P_{gen_{tot}}^{WG}}{P_{gen_{init}}^{CG} + \Delta P_{gen_{tot}}^{CG} + P_{gen_{tot}}^{WG}} \quad (3.6)$$

Where  $P_{gen_{tot}}^{WG}$  is the total power generated by the WGs,  $P_{dem_{tot}}$  is the total demanded power,  $P_{gen_{init}}^{CG}$  is the initial power generated by the CGs and  $\Delta P_{gen_{tot}}^{CG}$  is the change in the total power generated by the CGs as time passes. The Simulink constant block "pgenCGtot" has to be written to from the MATLAB script at every simulation when a different generator is shut off since the generated power by the CGs changes.

The WGs are mounted into groups, in such a way that the number of groups connected to the grid is a parameter. Two Simulink selector blocks specify the number of WGs to be connected. These two blocks are connected through an external port to a Simulink constant block "numWG" that specifies the indexes to pick from the multiplexer that stores the powers generated each WG group. The constant block is also written from the MATLAB script.

### 3.3.3 Storing and visualisation

The outputs obtained from the simulations are stored within five data structures of cell array type. These are called  $c\_t\_wg$  (storing time data),  $c\_w\_wg$  (for frequency data),  $c\_pufls\_wg$  (for shed power),  $c\_pgenWGtot\_wg$  (for power generated by the WGs),  $c\_WGpenetration\_wg$  (for WG penetration), and  $c\_pgenWGtot\_wg$  (for the total power generated in the system). Each data container (or cell) in these 5-dimensional data structures has an array of variable length. This data structure has been used precisely because of this variability in length of the outputs. It also allows easy access to this data, which is necessary for obtaining the indices of each simulation.

The steady-state frequency can easily be obtained by selecting the last element of each array from  $c\_w\_wg$ , while the nadir frequency has to be obtained by searching for the minimum frequency in the array, even though it significantly increases computation time. Similarly, to the steady-state frequency, the total shed power by the UFLS can be obtained by taking the last element of  $c\_pufls\_wg$ .

When these indices have been obtained, they are stored in three matrices. These three 5-dimensional matrices,  $m\_fss$ ,  $m\_fmin$  and  $m\_pufls$  only require one data element of fixed size, thus a multidimensional matrix is enough.

A set of special visualisation functions have then been made so as to be able to plot and see how the five outputs evolve in time, given a set of parameters. These functions also print out the indices on a LaTeX table so as to see the quantified indicators.

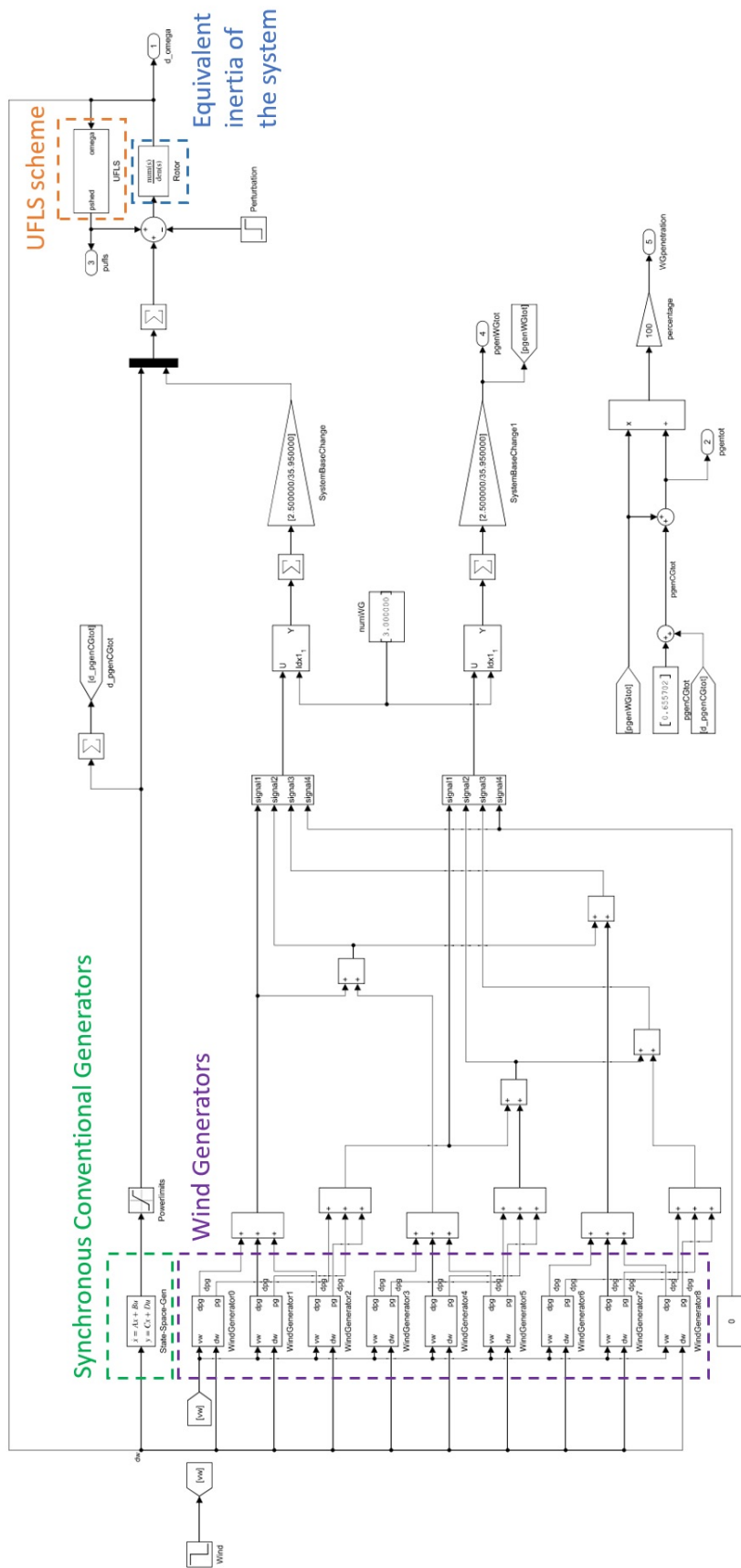


Figure 3.5: Simulink model of the power system.

### 3.4 Cost of implementation

The problem entails conducting a comprehensive set of simulations to assess the behavior of a power system under various scenarios. A standard computer, given enough time, can process these. A MATLAB license is needed as well as the Simulink software.

There are 24 generation scenarios considered, each involving the disconnection of 8 generators. Additionally, three different wind speeds are tested at three different times, while also exploring three different WG penetrations. By combining these parameters, a total of 1728 simulations need to be performed. The total computation time of these simulations amounted to 74 minutes on a laptop with an Intel core i7. The workspace storing all the results takes a total space of 29 MB.

# Chapter 4

## Analysis of results

In this section, we embark on the analysis of the results obtained from the time-domain MATLAB/Simulink simulations conducted to assess the impact of different wind generation penetrations on the frequency deviation of the power system. By scrutinizing the simulation outcomes, we aim to gain a deeper understanding of how the system's frequency response is influenced when a generator outage aligns with a decline in wind speed. This analysis provides valuable insights into the behavior and stability of the power system under varying scenarios, shedding light on the potential challenges and risks associated with integrating wind power.

### 4.1 Base case

In this subsection, the analysis focuses on the results of the base case simulation, considering the loss of a generator without any wind speed change. The outcomes of this scenario in the time-domain MATLAB/Simulink simulation are examined to establish a baseline understanding of the power system's frequency deviation behavior under the condition of a generator outage. This allows for the isolation of the impact of the generator loss on the system's frequency response, independent of wind speed variations. Through this analysis, valuable insights are gained regarding the system's ability to maintain stability and regulate frequency in the absence of a specific wind-related disturbance. These findings serve as a reference point for comparison when investigating the combined effect of wind speed changes and generator outages in subsequent subsections.

#### 4.1.1 Scenarios

In the context of the project, certain scenarios, especially scenarios 1 to 4, hold particular significance. The three WGs groups are simulated here. An advantage to compare these four scenarios is that they each involve a decreasing WG generation (from a total of 10 MW down to 5.3 MW), allowing for an evaluation of the impact on the total power generated by the WGs. The same CG is being disconnected in each of these scenarios and almost all the other CGs generate the same active power. This facilitates the analysis of the power generated by the WGs with little correlation to other parameters. Additionally, choosing only these four scenarios allows us to visualise the results on a single plot. These aspects thus provide valuable insights into understanding the relationship between WG generation, power output, and system stability.

[Figure 4.1](#) shows how different variables of the power system react when CG 21 is shut down. The frequency response, the shed load, the percentual WG penetration, the WG power and the total power generation is shown in a 25 seconds timeframe. Additionally, [Table 4.1](#) summarises the stability of the system by showing the steady-state frequency, the frequency nadir and the total shed power for the different scenarios. It can be seen that the UFLS scheme is activated in every scenario. This is due to the fact that the outage of the CG at bus 21 is simply is very large. For all scenarios, it initially represents 20 to 25% of all the generated active power. Nonetheless, the shed power is considerably higher in scenarios 3 and 4. Due to this shedding, they do end up having a lower deviation from the nominal frequency.

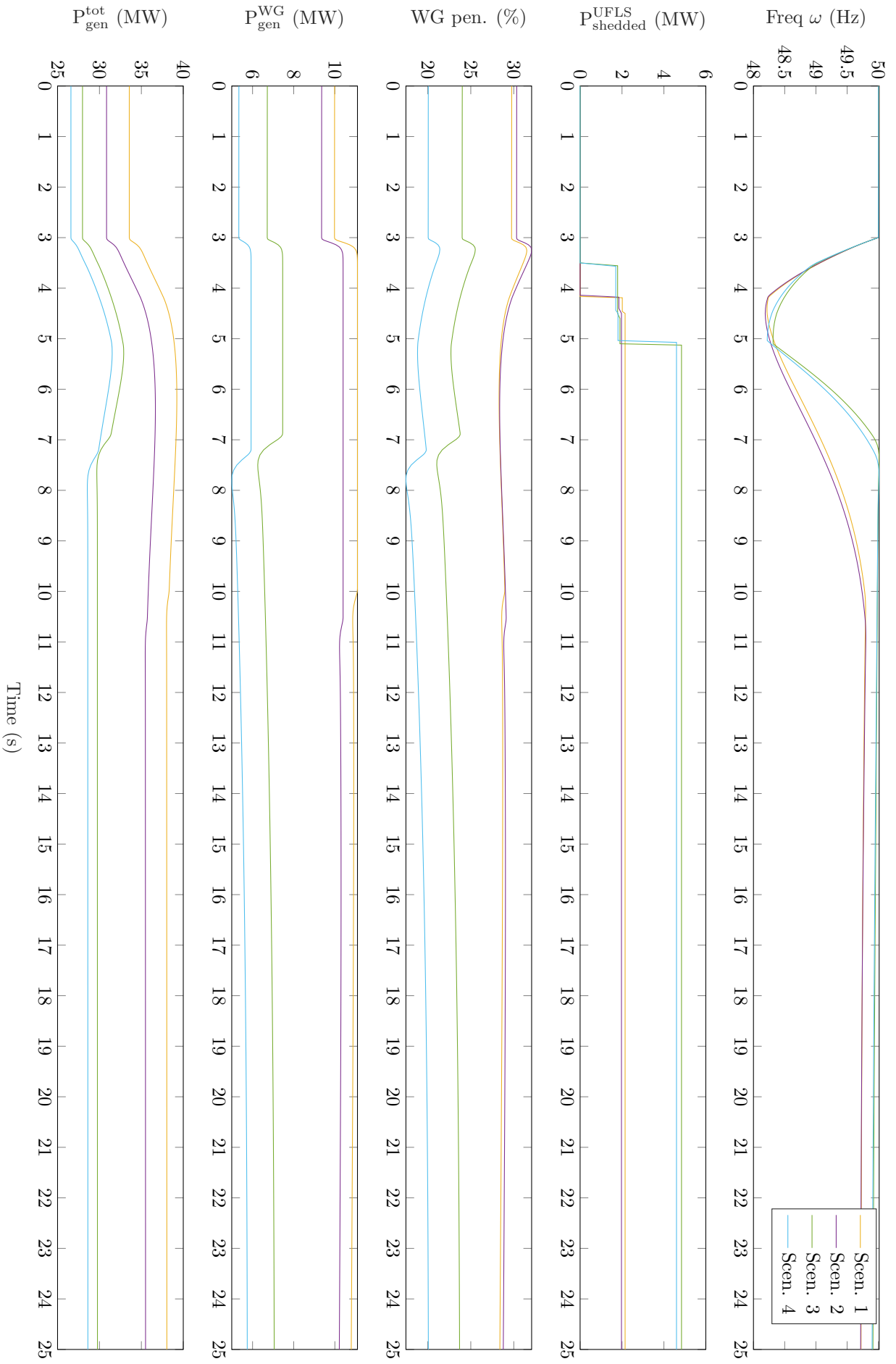


Figure 4.1: Simulation of scenarios 1 to 4 showing the frequency response when CG 21 is lost. There are 9 WGs connected.

When the frequency event occurs at the third second, it can be seen how the WGs make use of their power margin thanks to the deloading by increasing their power output. Nonetheless, scenario 1 and 2 must use this power reserve for a longer period of time before going back to the new equilibrium. This is because these two scenarios shed less load, thus they take more time to reach a steady-state. The total power generated by the system increases due to the primary frequency regulation carried out by the WGs but most importantly, the CGs (e.g. in scenario 1, around 20% of the added generated power in steady-state came from the WGs). The combination of all these phenomena causes the percentual WG penetration to evolve as a U-shape for the first few seconds of the frequency event.

It is worth noting that in scenarios 3 and 4, the power generated by the WGs actually becomes lower than the initial generated power at some instants (approximately in the time range between 7.5 and 10 seconds). This is due to the abrupt actuation of the UFLS scheme and its resulting momentary frequency increase over the nominal frequency.

Table 4.1: Indices of the base case for scenarios 1 to 4 with the loss of CG 21.

Scenario	$f_{ss}(Hz)$	$f_{min}(Hz)$	$P_{ufls}(MW)$
1	49.7223	48.2169	2.1479
2	49.7160	48.1883	1.9742
3	49.9130	48.3135	4.8402
4	49.8995	48.2207	4.6011

### 4.1.2 Generator lost

This section considers the impact of losing different generators for scenario 1. Constant wind speed is assumed here as well. The three WG groups are also being considered here to simulate a system with high wind energy penetration.

As can be seen from [Figure 4.1](#) and [Table 4.2](#), the UFLS scheme is put into use when the CGs 17 and 21 are lost. This is not surprising since they represent 27 and 20% of the initial total power generation, respectively. Additionally, due to this difference in their power contribution, the simulation where CG 17 is lost sheds more than three times the power than the other case where CG 21 is disconnected. Nonetheless, this causes the frequency nadir of simulation CG 21 to reach a considerably lower value (48.2 rather than 48.6 Hz). This is also why the CGs where CG 21 is lost are forced to produce more total power and the WGs produces power for several seconds longer than when CG 17 is lost.

On the other hand, the first three simulations where CGs 12, 13 and 15 are disconnected show a satisfactory action of the primary frequency regulation. The UFLS scheme does not shed load, the frequency nadir does not go beyond 49.2 Hz and the steady-state only deviates by at most 0.2 Hz.

Table 4.2: Indices of the base case for scenario 1 with the loss of each CG. Note that the outputs are the same when CG 12 and 13 are lost. This is because they have the same generator specifications and they initially produce the same power.

Lost CG	$f_{ss}(Hz)$	$f_{min}(Hz)$	$P_{ufls}(MW)$
12	49.8613	49.5910	0.0000
13	49.8613	49.5910	0.0000
15	49.8036	49.2183	0.0000
17	49.8667	48.6263	6.9471
21	49.7223	48.2169	2.1479

### 4.1.3 Effect of the droop control

It is of interest to examine what the effect of the droop control has on the operation of the WGs and the power system as a whole. This can be changed in the model by setting the droop parameter  $R$



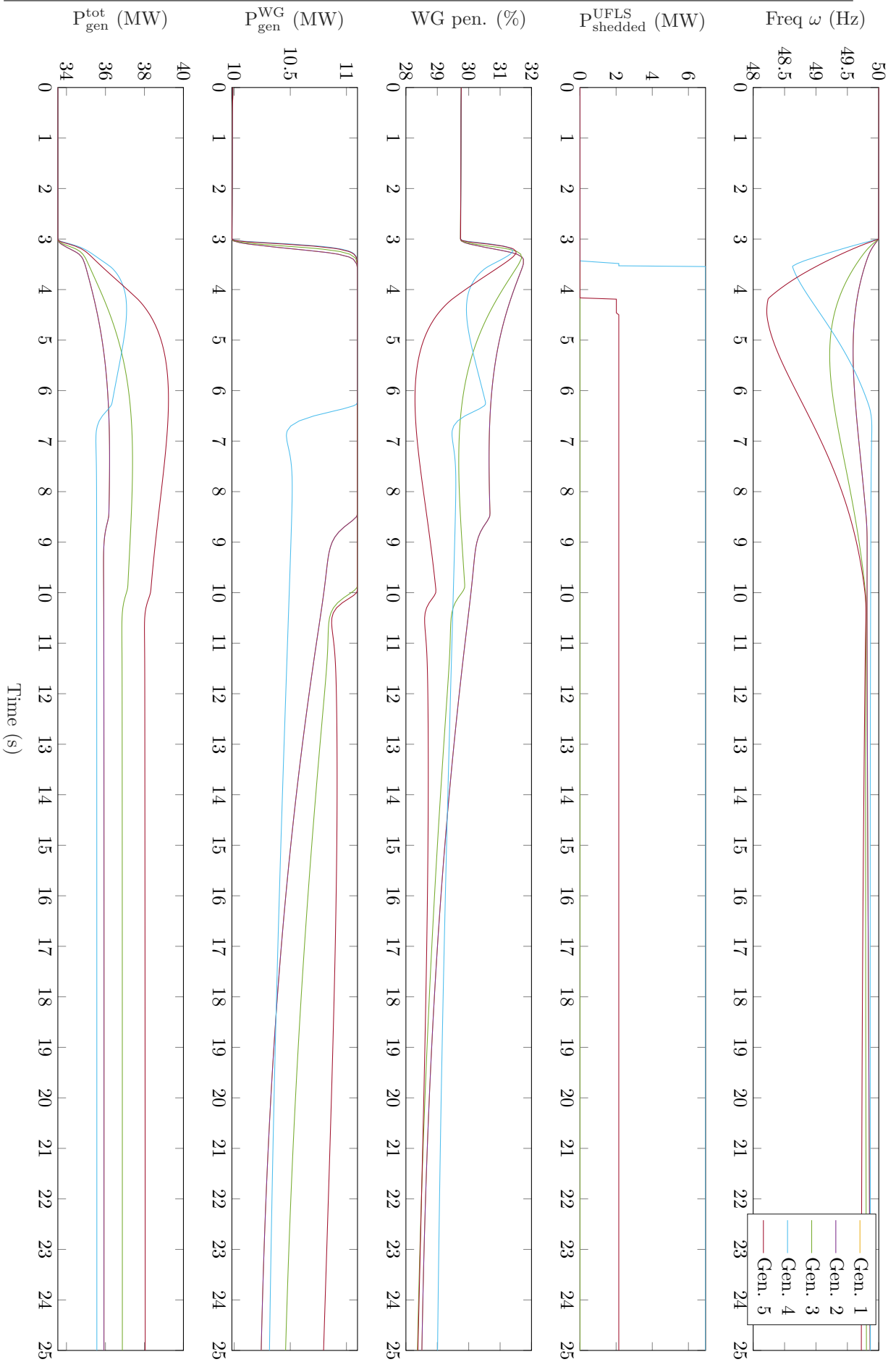


Figure 4.2: Simulation of scenario 1 with each CG getting lost in  $t = 3$  s. There are 9 WGs connected.

to a very large number to cancel droop control. In this particular case, scenario 1 will be examined. The simulation takes into account 9 WGs and no wind speed drop.

The simulation output can be seen in [Figure 4.3](#). It can be observed that while not having a droop controller might be better for the frequency nadir, it is not the case for the power shed by the UFLS scheme, as shown in [Table 4.3](#). In the case of the WGs with droop, the power generated by them increases by about 10%, as expected by their deloaded operation mode. This is not the case for the WGs with no droop. There is no primary regulation so their power output remains the same (it is assumed that the small deviation simply comes from the inaccuracy related to the look-up tables). The reason for having higher frequency nadir values without droop is that more load is shed due to the activation of the underfrequency and ROCOF stages of the UFLS scheme, whereas with droop only underfrequency stages are activated.

Table 4.3: Indices of scenario 1 with the loss of CG 21, with and without a droop controller.

	$f_{ss}(Hz)$	$f_{min}(Hz)$	$P_{ufls}(MW)$
Droop	50.0167	48.2169	2.1479
No droop	49.7223	48.7956	6.9471

## 4.2 Sensitivity analysis

This section delves into the evaluation of critical factors, namely wind speed, timing of the wind speed changes relative to frequency events, and the penetration level of WGs. This analysis aims to discern the impact of these parameters on the dynamic behavior of the power system. By methodically varying these factors in our simulations, we can gain valuable insights into how the system's response to frequency events is influenced. Understanding the sensitivity of the system to changes in wind speed, timing, and WG penetration is crucial for optimizing the stability and reliability of power systems operating with a high proportion of wind generation.

### 4.2.1 Wind generator penetration

It is of interest to evaluate the simulation for different WG penetrations since this parameter might affect the reliance of the stability of the power system on the wind speed. By adjusting the WG penetration and observing the resulting frequency deviations, some insight can be gained regarding the interplay between WG penetration, system stability, and the power system's response during the outage of a generator.

The third scenario where CG 15 gets shut down is evaluated. The wind speed drops by 1 *m/s* at the time of the frequency event.

It can be seen from [Table 4.4](#) that the more WGs connected, the lower the value at the frequency nadir is. This shows that the system becomes more dependent on wind variability even with WGs capable of primary frequency regulation. It can be seen in [Figure 4.4](#) that the WGs decrease their reference power at the time of the frequency event.

The three simulations explored here each shed more load than the next as seen in [Table 4.4](#). However it should be noted that this difference in shed loads simply resides in the fact that the initial generated power is different. Since the demand must be equal to the generation, the power demanded by the grid is largest when all three WG groups are connected. Since the power shed by the UFLS scheme is proportional to this demand, the absolute numbers in MW will be different. It can thus be seen that, in all three cases, the same UFLS scheme in substation 2101 is put into action by shedding 6% of the initial load. This difference in shed power also causes the three simulations to have different steady-state frequencies.

What is unequivocal independently of the percentage in demand shed is the timing at which it happens. As there are more WGs, the system relies more on the wind speed. When this parameter decreases in value, this causes the UFLS scheme to activate sooner.

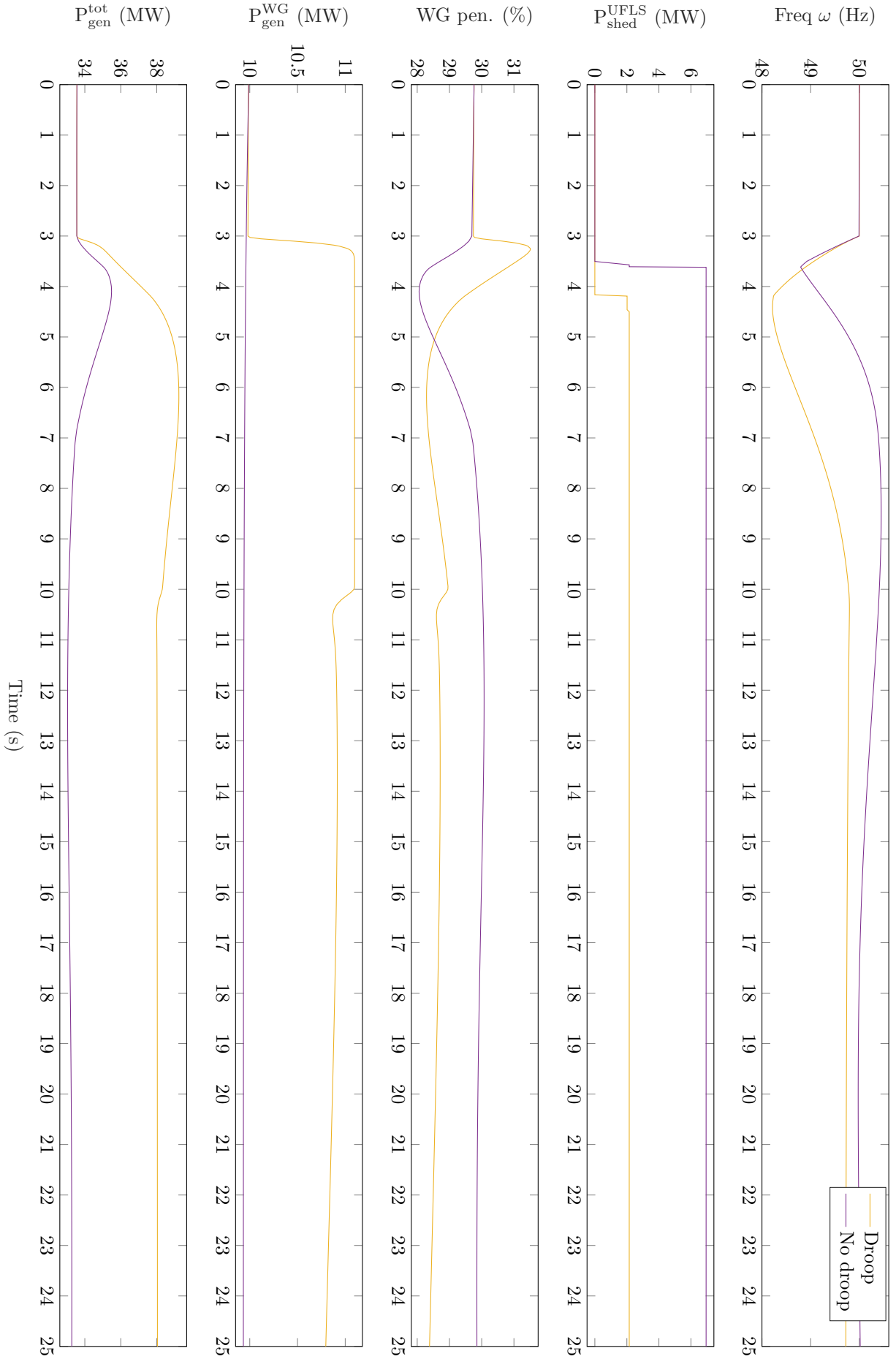


Figure 4.3: Simulation of scenario 1 with CG 21 getting lost in  $t = 3$  s, with and without droop control. There are 9 WGs connected.

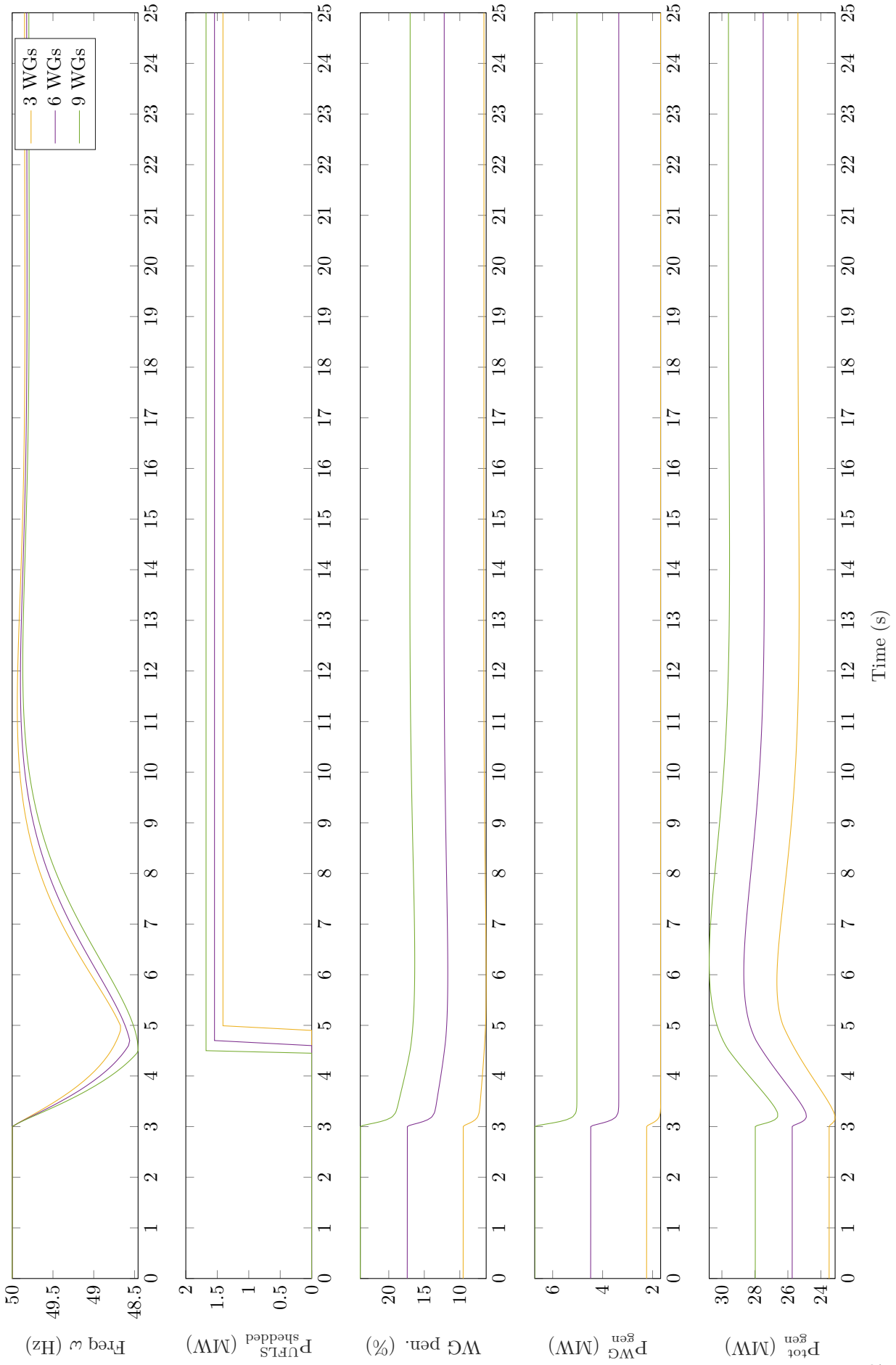


Figure 4.4: Simulation of scenario 3 for multiple wind energy penetrations with CG 15 getting lost at  $t = 3$  s.

Table 4.4: Indices for scenario 3 with the loss of CG 15.

$n^{\circ}$ of WGs	$f_{ss}(Hz)$	$f_{min}(Hz)$	$P_{ufls}(MW)$
3	49.8489	48.6721	1.4099
6	49.8223	48.5591	1.5443
9	49.7958	48.4566	1.6787

### 4.2.2 Wind speed change

Scenario 2 is interesting to study because it has the largest initial wind energy penetration (it being 30% when nine WGs are connected).

In Table 4.5 can be seen that all scenarios cause the actuation of the UFLS scheme. Nonetheless, this is mostly due to the nature of the frequency event, not the change in wind speed. This can be confirmed by seeing how some load is shed even though there is no drop in wind speed. In fact, it may seem like a drop in wind speed is better for the stability because the frequency at the nadir is higher then. However, the only reason why this happens is because there is more load shed when load is disconnected.

As usual, when there is no wind speed change, the WG uses its deload power to compensate for the loss of the generator. However, when there is a drop in wind speed, the deloaded operation mode sets a new power reference. This corresponds to the blue curve in Figure 3.2. When the wind speed decreases by 0.5 m/s, this new reference is the MPP at the 8.55 m/s curve (generating 0.39 pu units at the rotor speed of 0.74 pu units in the WG in Figure 3.2). When the frequency has been stabilised by the load shedding and the actuation of the primary frequency regulation of the other CGs, this power reference is allowed to decrease. This is not the case for a wind speed drop of 1 m/s, where the power reference drops to 7.32 MW. In Figure 3.2, that quantity represents 0.325 pu units. This is the MPP of the 8.05 m/s curve.

Table 4.5: Indices of simulation for scenario 2 with the loss of CG 17.

$\Delta v_w(m/s)$	$f_{ss}(Hz)$	$f_{min}(Hz)$	$P_{ufls}(MW)$
0	49.9271	48.3531	5.3367
0.5	49.8672	48.6695	6.3855
1	49.8170	48.4536	6.3855

### 4.2.3 Timing of the wind change

The purpose of this particular sensitivity analysis is to analyse the timing of the wind speed drop. The focus is on examining the precise moments at which changes in wind speed coincide with frequency events in the power system. The effects of wind speed variations occurring 2 seconds before, after, and exactly when the frequency event occurs are investigated to gain insights into the system's response and potential instabilities. This analysis allows for an understanding of the time-dependent dynamics of the power system and how closely aligned wind speed fluctuations with frequency events can influence system stability. By assessing the timing of the wind speed drop, a better comprehension of the critical time windows that significantly impact the overall behavior of the power system can be achieved, enabling informed decisions to enhance its resilience and reliability. The scenario 21 with the CG 11 lost is discussed here. It is of interest to see how the frequency might become affected by purely the timing of generator outage with regards to the drop in wind speed and not from the UFLS scheme. This way, the frequency nadir in particular can be better evaluated.

The simulation outputs in Figure 4.6 and Table 4.6 show that the frequency at the nadir reaches its lowest point when the wind speed drop occurs at the same time as the frequency event. Otherwise, this same value does not vary considerably whether the wind drops two seconds before of after the generator outage. The steady-state frequency is quite similar and would become the same value if given enough simulation time. This is because the steady-state can be obtained by simply power imbalances, and these imbalances are the same in all the three cases in this analysis. This is also

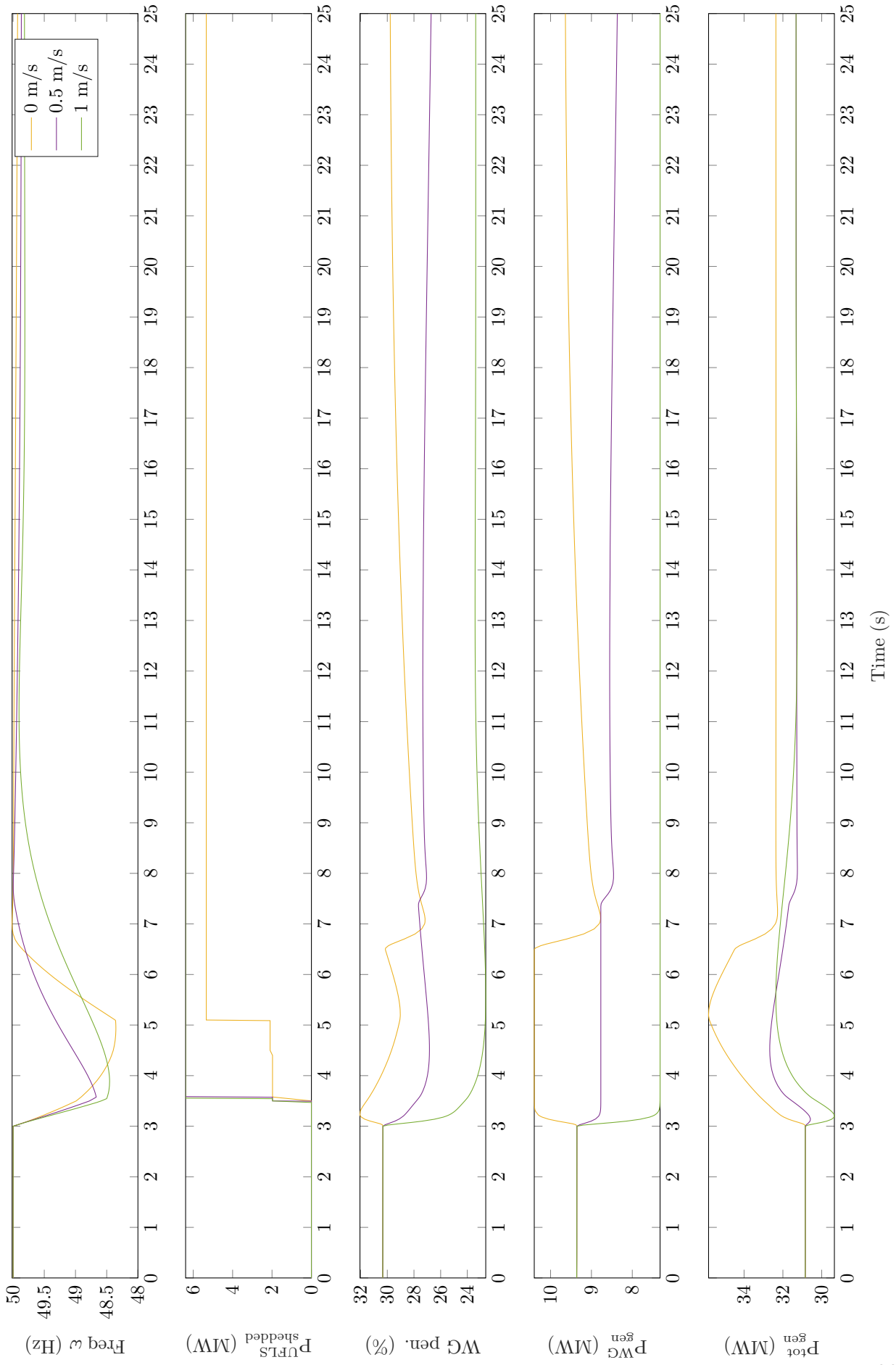


Figure 4.5: Simulation of scenario 2 with a starting wind speed of 9.05 m/s for different wind speed drops at the same time as the frequency event. There are 9 WGs connected.

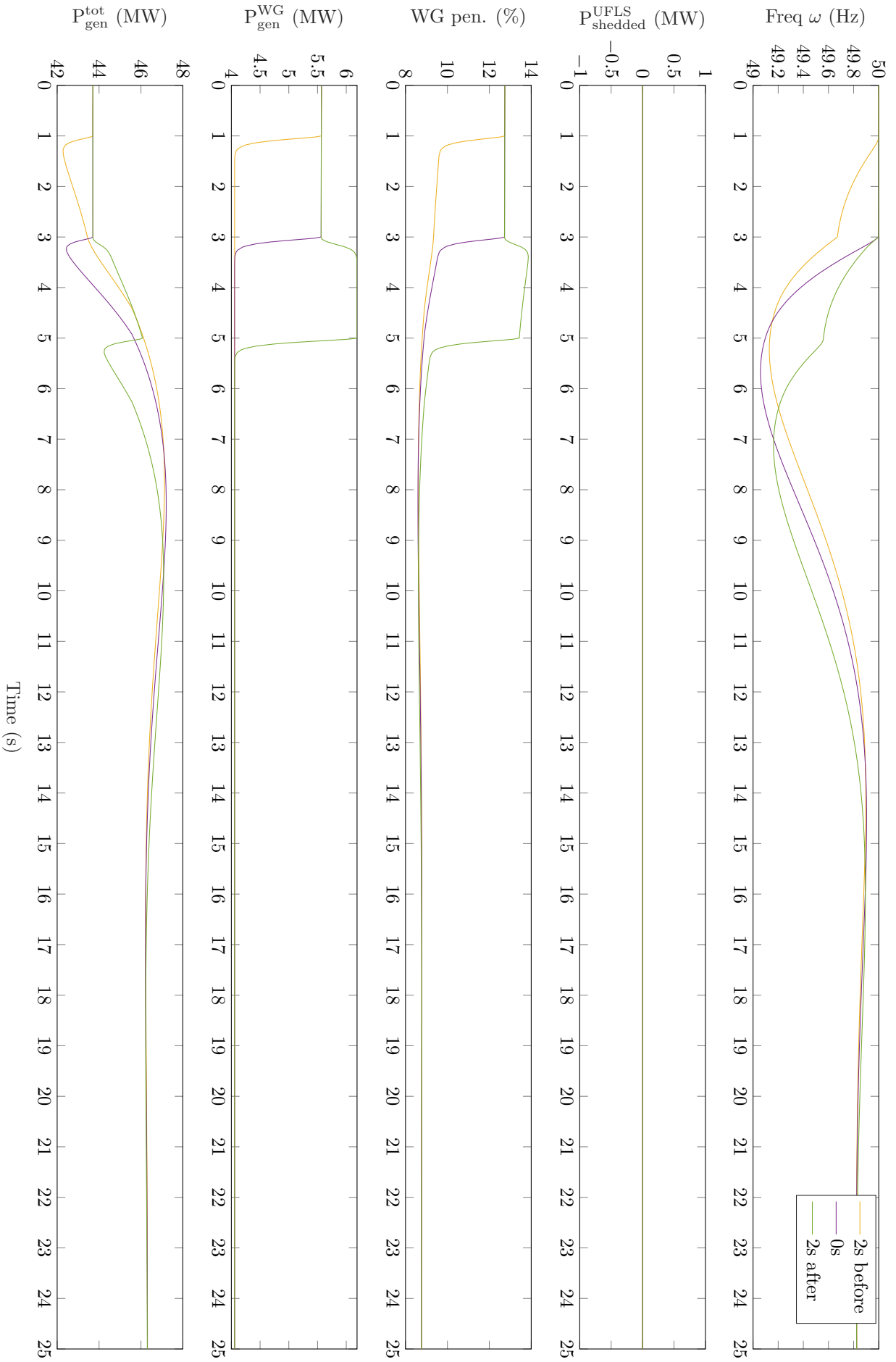


Figure 4.6: Simulation of scenario 21 for different times at which the wind speed drops relative to the frequency event. There are 9 WGs connected.

portrayed in the other time-domain simulations of [Figure 4.6](#) when the generated power by the WGs, the total power generated and the WG penetration all end to essentially the same value.

In the steady-state, the power generated by the WGs decreases to the same reference point no matter when the wind speed decreases. This is no surprise as explained earlier. However, in the case where the wind speed drops after the frequency event, the reference power is momentarily set to the MPP of the corresponding initial wind speed of 5 m/s. Two seconds after the generator outage, the power drops to the MPP of the 4 m/s curve, along with the other simulations.

Table 4.6: Indices of simulation for scenario 21 with the loss of CG 1.

$\Delta t_{\Delta v_w}(s)$	$f_{ss}(Hz)$	$f_{min}(Hz)$	$P_{ufls}(MW)$
-2	49.8255	49.1292	0.0000
0	49.8243	49.0593	0.0000
+2	49.8239	49.1629	0.0000

#### 4.2.4 Sensitivity analysis on all simulations

The overall effect of the number of WGs, the change in wind speed, and the time at which it happens can be quantified as well. An overall sum of the shed power and the maximum deviation of the frequency for all simulations taking into account only one particular parameter can be executed.

[Table 4.7](#) shows how, as the WGs in the system increases, the frequency nadir and the shed power worsens. It is worth mentioning that these sums include the simulations where the wind speed does not vary, thus this reflects less variation between the results.

Table 4.7: Sums of the shed power and maximum deviations from the base frequency from all simulations, depending on number of WGs in the system.

	3 WGs	6 WGs	9 WGs
$\Sigma P_{ufls}$	2172.1	2408.2	2617.5
$\Sigma \Delta f_{min}$	1450.4	1468.4	1504.7

On the other hand, [Table 4.8](#) shows how, as the wind speed change increases, so does the shed power by the UFLS and the frequency deviation from the base frequency. This clearly shows that generally speaking, the more wind speed change there is, the more unstable the system becomes.

Table 4.8: Sums of the shed power and maximum deviations from the base frequency from all simulations, depending on the wind speed change.

	0 m/s	0.5 m/s	1 m/s
$\Sigma P_{ufls}$	2084.5	2327.5	2785.8
$\Sigma \Delta f_{min}$	1338.9	1479.9	1604.6

On the other hand, [Table 4.9](#) shows these same sums but with the timing of the wind speed change as a parameter. It can be seen that, generally speaking, the system is more unstable when the wind slows down right when the frequency event occurs. Additionally, this system shows that more load is shed when the wind slows 2 seconds before the generator loss than after, thus its frequency deviation reaches less extreme values.



Table 4.9: Sums of the shed power and maximum deviations from the base frequency from all simulations, depending on the time of the wind speed change.

	-2 s	0 s	+2 s
$\Sigma P_{ufls}$	2381.8	2470.8	2345.2
$\Sigma \Delta f_{min}$	1486.6	1502.0	1434.8

# Chapter 5

## Conclusions

### 5.1 Conclusions on the methodology

A model of a WG has been developed. In order for it to provide primary frequency regulation, it needed to generate less power than the one it could immediately provide, i.e. it needed to operate in a deloaded rather than an MPPT operation mode. It was deemed appropriate to control this power through variable rotor speed control. By making use of a deloaded control, an added additional power reference could be adequately added. This power reference comes from a droop control depending on the frequency variation. The combination of these controls are not dependent on the type of WG. The developed model represents the dynamics of the rotor, whereas MPPT and deloaded operations modes were described by means of simplified look-up tables. The integration of the mechanical and the electrical part of WG system was assimilated, thus completing the WG model.

The WG model was integrated into a power system model. Multiple of these generators were added so as to make them represent a considerable part of the grid's generation, i.e. have a large wind energy penetration. Even though the end objective is to evaluate the frequency and the shed load in the system, other outputs such as WG generation and total generation were added. This allows for a more hollistic visualisation of why the frequency behaves the way it does. Many parameters were added to the Simulink model. The initial deloaded power generated by the WGs was read from an Excel file for every scenario and its corresponding initial wind speed was calculated and set. The power generated by the CGs was also read for every scenario. All the wind parameters and the number of connected WGs were iteratively changed and selected. These simulations could of course not have been undertaken if the Simulink model were not coordinated with a MATLAB script that sets these parameters correctly for every simulation.

### 5.2 Conclusions on the results

It has been shown that the deloaded operation mode and the additional droop action benefit the power system (i.e. lower the shed demand) when there is no variation in wind speed. The extra power generated by the WG helps close the unbalance between the generation and demand. However, when speed variations are considered, these controls are not actually able to compensate for the generator loss even when they try to fully use their instantaneous power reserve.

When evaluating the overall sums of demand shed and frequency deviations for all possible simulations, it can be seen that as more WGs are integrated into the system, the more unstable it becomes. Additionally, as the wind speed change increases, the system gets more unstable as expected. Another observation is that the instant at which the wind speed drop occurs is not as relevant as the other parameters. Nonetheless, the system reaches a more critical level when the wind speed drops at the same time as the frequency event.

When examining the first few different scenarios in this specific island system, it can be seen that the UFLS scheme is activated in all cases. This is due to the fact that the generator that is lost is very large. It is important to realise that the dependency on a single CG for a significant portion of

power generation diminishes the significance of installed WGs in providing primary frequency regulation. In such cases, regardless of the WG's capacity for frequency control, the focus shifts towards the critical factor of load shedding. Nevertheless, it is important to acknowledge that the extent of load shedding must be considered. However, the ideal objective should be to prevent such scenarios from occurring in the first place. By implementing robust measures and strategies to ensure a well-balanced and reliable power system, the need for significant load shedding can be minimized or even eliminated.

The CG lost in the system has a clear impact on how much load is shed. In scenario 1, losing one generator can cause three times more load shedding than getting another generator shut down. Their relevance is so large that even when there is load shedding, their frequency at the nadir reaches further down values than when the three other CGs are disconnected.

It has been shown that the wind energy penetration affects the stability of the system. Even though it is seen that the WGs try to provide more power and thus make the system more stable, it does not necessarily have enough power reserve to avoid the action of the UFLS scheme. The effect on frequency stability is similar when 3, 6 or 9 WGs are connected. However, as already discussed, this is mainly due to the fact that the shed load is set as a percentage of the demand. Each of these simulations start with a different generation, and thus different demands, so that when a load is shed, the absolute value of this quantity in MW is different.

Additionally, it has been shown that, as expected, a wind speed drop worsens the stability of the system by increasing the load shed. It is possible that a drop in wind speed may result in a higher frequency nadir. However, this effect is attributed to the increased shedding of load during such events, which is comparatively more relevant.

It is possible to learn more about the dynamics and stability of the system by looking at different timings at which the wind speed drops in relation to the frequency event. The results show that when the wind speed drops and a frequency event occurs simultaneously, the frequency nadir is at its lowest. However, the frequency response is not significantly affected by whether the wind speed drop occurs 2 seconds before or after the occurrence.

### 5.3 Recommendations for future research

This project can be improved further by a better modelling of the WG. A pitch angle controller can be integrated into the model so as to make a better and more realistic rendition of today's WGs. Additionally, this would have permitted a more thorough investigation in which the magnitude of the wind speeds are higher. A stall control could have been also implemented in addition or instead of the pitch angle controller. The model used in this project is also idealised in the sense that it is assumed that the rotor speed is measured continuously and with exact precision. A noise with realistic magnitude could be added to represent this uncertainty in measurement. Additionally, a discretised model would be applicable, where the rotor speed is measured with a corresponding sampling frequency. A state observer would be applicable for estimating the rotor speed as well.

The modelling of the wind can be improved. As discussed previously, the power system model includes several instances of the same WG. The current model could have been simplified so that only one WG is needed and its outputs are simply multiplied by the number of WGs in the system. This would have been beneficial in order to use less computation time. However, it was set in this way on purpose since it could be of interest to apply a different wind pattern to each of these generators. It is assumed in this model that the wind would be similar in all the WG locations throughout the island, however, if the island is large enough, this assumption cannot be made anymore. The wind applied to each WG could have a delay or have completely different noise levels altogether. The aerodynamics of the blades, even though it is widely used in current literature, could be even more precise. An array of wind signals could have been created so that the impact of it against the blades at different altitudes can be modelled.

The control action implemented in this project only responds to the change in wind speed and to the frequency deviation. It would be of great interest to implement a control whose intention would be to increase the power output when it is inevitably reduced. If a frequency event occurs whilst operating in the deloaded mode at a constant wind speed, the rotor speed slows down. Nonetheless, according to the deloaded operation mode the power output would decrease.

If a pitch angle controller is added to the modelling of the WG, it would also have been interesting to set more aspects of the wind as parameters. In this project, the wind speed is set by the power generated by the WGs. But for instance, the opposite could also have been explored. Other examples of parameters could be: variability of the wind speeds among the WGs, an inter-delay between them, rate of change of wind speed (rather than using a step function), and more.

The analysis of the results can be explored further. The frequency nadir, its steady-state and the load power shed were explored. However, the ROCOF could be looked into as well. This would involve calculating the slope (or difference in frequency) in the corresponding arrays when the frequency changes severely. This would inform how severe the transient response would be. From the results obtained, a more concise conclusion could have been elaborated in such a way that an overall ‘score’ can be given to the stability of the grid. This would involve assigning weights to the different indicators, such as the frequency nadir and the shed load. However this would be challenging to implement. The grid must without question require that no load shedding is carried out at all times and that the frequency does not go beyond 48 Hz. In extreme situations where these points are reached, it may make little sense to assign in such binary requirements.



# Chapter 6

## Appendix

### 6.1 Data and specifications

Table 6.1: Generation scenarios.

	<b>11</b>	<b>12</b>	<b>13</b>	<b>14</b>	<b>15</b>	<b>16</b>	<b>17</b>	<b>18</b>	<b>19</b>	<b>20</b>	<b>21</b>	<b>22</b>
<b>1</b>	0.00	2.35	2.35	0.00	3.30	0.00	8.94	0.00	0.00	0.00	6.63	0.67
<b>2</b>	0.00	2.35	2.35	0.00	3.30	0.00	6.86	0.00	0.00	0.00	6.63	0.62
<b>3</b>	0.00	2.35	2.35	0.00	3.30	0.00	6.63	0.00	0.00	0.00	6.63	0.45
<b>4</b>	0.00	2.35	2.35	0.00	3.30	0.00	6.63	0.00	0.00	0.00	6.63	0.36
<b>5</b>	0.00	2.35	2.35	0.00	3.30	0.00	6.63	0.00	0.00	0.00	6.63	0.37
<b>6</b>	0.00	2.35	2.35	0.00	3.30	0.00	6.63	0.00	0.00	0.00	6.63	0.49
<b>7</b>	0.00	2.35	2.35	0.00	3.30	0.00	8.63	0.00	0.00	0.00	6.63	0.45
<b>8</b>	2.35	2.35	2.35	0.00	3.30	0.00	9.38	0.00	0.00	0.00	6.63	0.45
<b>9</b>	2.35	2.35	2.35	2.82	3.30	0.00	10.86	0.00	0.00	0.00	6.63	0.42
<b>10</b>	2.35	2.35	2.35	2.82	3.30	0.00	8.82	0.00	0.00	6.63	6.63	0.29
<b>11</b>	2.35	2.35	2.35	2.82	3.30	0.00	10.08	0.00	0.00	6.63	6.63	0.22
<b>12</b>	2.35	2.35	2.35	2.82	3.30	0.00	9.38	0.00	0.00	6.63	6.63	0.21
<b>13</b>	2.35	2.35	2.35	2.82	3.30	0.00	9.46	0.00	0.00	6.63	6.63	0.20
<b>14</b>	2.35	2.35	2.35	2.82	3.30	0.00	10.04	0.00	0.00	6.63	6.63	0.18
<b>15</b>	2.35	2.35	2.35	2.82	3.30	0.00	9.01	0.00	0.00	6.63	6.63	0.17
<b>16</b>	2.35	2.35	2.35	0.00	3.30	0.00	9.53	0.00	0.00	6.63	6.63	0.18
<b>17</b>	2.35	2.35	2.35	0.00	3.30	0.00	8.21	0.00	0.00	6.63	6.63	0.19
<b>18</b>	2.35	2.35	2.35	0.00	3.30	0.00	8.26	0.00	0.00	6.63	6.63	0.21
<b>19</b>	2.35	2.35	2.35	0.00	3.30	0.00	10.32	0.00	0.00	6.63	6.63	0.21
<b>20</b>	2.60	2.60	2.60	0.00	5.78	0.00	11.20	0.00	0.00	6.63	6.63	0.25
<b>21</b>	2.60	2.60	2.60	0.00	5.89	0.00	11.20	0.00	0.00	6.63	6.63	0.37
<b>22</b>	2.35	2.35	2.35	0.00	4.23	0.00	11.20	0.00	0.00	6.63	6.63	0.49
<b>23</b>	2.35	2.35	2.35	0.00	3.30	0.00	7.71	0.00	0.00	6.63	6.63	0.54
<b>24</b>	2.35	2.35	2.35	0.00	0.00	0.00	6.63	0.00	0.00	6.63	6.63	0.50

Bus	11	12	13	14	15	16	17	18	19	20	21	22
k (on MBASE, =1/R)	20.00	20.00	20.00	20.00	20.00	20.00	20.00	21.25	20.00	20.00	20.00	20
H (s) (on MBASE)	1.75	1.75	1.75	1.73	2.16	1.88	2.10	6.50	2.10	2.10	2.10	5
MBASE (MVA)	5.4	5.4	5.4	6.3	9.4	9.6	15.75	26.82	14.5	14.5	14.5	1.5
Pmax (MW)	4	4	4	4.5	7	7	12	22.8	12	12	12	1.5
Pmin (MW)	2.5	2.5	2.5	3	3.5	3.5	7	0	7	7	7	0.00
B1	1.82	1.82	1.82	1.80	3.16	2.05	3.21	0.83	3.21	3.21	3.21	0
B2	0.00	0.00	0.00	0.00	0.00	0.00	0.00	0.00	0.00	0.00	0.00	0
A1	17.31	17.31	17.31	17.11	25.03	18.88	25.32	5.20	25.32	25.32	25.32	1
A2	0.79	0.79	0.79	0.85	9.80	1.68	9.70	3.40	9.70	9.70	9.70	0

Generator specifications.

Type	Substation	Freq. (Hz)	ROCOF (Hz/s)	Intentional delay (s)	Opening delay (s)	load (%)
uf	2101	48.81	0.30	0.20	0.20	6.00
uf	2102	48.81	0.60	0.20	0.20	0.40
uf	3101	48.66	1	0.2	0.2	10.5
uf	3102	48.66	1.5	0.2	0.2	3.8
uf	2103	48.66	2	0.2	0.2	7
uf	1101	48.00	0.80	0.20	0.20	17.40
uf	1111	48.00	1.50	0.20	0.20	8.70
uf	3103	47.00	1.80	0.20	0.20	12.30
uf	3104	47.00	2.10	0.20	0.20	11.50
uf	1102	47	2.4	0.2	0.2	2.2
uf	1112	47	2.4	0.2	0.2	7.8
rocof	2101	49.5	0.1	0.2	0.2	6
rocof	21020	49.5	0.1	0.2	0.2	0.4
rocof	3101	49.3	0.1	0.2	0.2	10.5
rocof	3102	49.3	0.1	0.2	0.2	3.8

UFLS scheme specifications.

## 6.2 Code

### 6.2.1 Main file

```

1 function main_rundynamicsimulation
2
3 %
4 % -----
4 % Predefined values
5 %
5 % -----
6
6 tic
7
8 powersystemdl = 'Powersystem.slx';
9 load_system('Powersystem');
10
11 str_uftype     = 'uf';
12 str_rocoftype  = 'rocof';
13
14 fbase          = 50;
15 tsimulation    = 25;
16 t0             = 3;
17 numWG         = 9;
18
19 % Choose here the number of scenarios to run (from scenario 1 to '
20 %   nscenarios')
20 nscenarios     = 24;
21
22 %
22 % -----
23
23 % Read input data
24 %
24 % -----
25
26 disp('Reading data...');
27
28 xlsfilename = 'LaPalmaInputData_noESS_withoutFCUC.xls';
29 [status, c_sheets] = xlsfinfo(xlsfilename);
30
31 % read generator dynamic model data
32 m_gendata     = xlsread(xlsfilename,c_sheets{1});
33
34 % read generation scenarios
35 m_genscenarios = xlsread(xlsfilename,c_sheets{3});
36 m_genscenarios = m_genscenarios(2:end,2:end); % delete first row and
37 %   column
38
38 v_pwg        = m_genscenarios(:, size(m_genscenarios,2)); % vector
39 %   storing power generated by WGs in each scenario
39 m_genscenarios = m_genscenarios(1:end,1:end-1); % delete last column
40
41 % correct max and min generation output

```



```

42 ngen = size(m_gendata,2)-1; % the '-1' is there to ignore the WG column
43 for igen = 1:ngen
44     v_idxcommitted = find(m_genscenarios(:,igen)>0);
45     m_gendata(6,igen) = min([m_genscenarios(v_idxcommitted,igen);
46         m_gendata(6,igen)]); % pmax
47     m_gendata(5,igen) = max([m_genscenarios(v_idxcommitted,igen);
48         m_gendata(5,igen)]); % pmin
49 end
50 % Read Nominal Power of WG
51 Pn = m_gendata(5,ngen+1);
52 diameter = m_gendata(11,ngen+1);
53 R = 1/m_gendata(2,ngen+1);
54 Hw = m_gendata(3,ngen+1);
55 % read ufls parameters
56 [m_uflsparam,c_uflsID] = xlsread(xlsfilename,c_sheets{4});
57 [m_ufparam , m_rocofparam, v_pshed0] = ...
58     fun_prepareuflsformat4simulinkformat(m_uflsparam, c_uflsID,
59         str_uftype, str_rocoftype);
60 v_dfufpu = (m_ufparam(:,1)-fbase)/fbase;
61 v_tintuf = m_ufparam(:,3);
62 v_topnuf = m_ufparam(:,4);
63
64 v_dfrocofpu = (m_rocofparam(:,1)-fbase)/fbase;
65 v_dfdtrocofpu = m_rocofparam(:,2)/fbase;
66 v_tintrocof = m_rocofparam(:,3);
67 v_topnrocof = m_rocofparam(:,4);
68
69 %
70 -----
71 % Simulate all possible single generating unit outages
72 %
73 -----
74
75 disp('Simulation start...');
76
77 m_genscenarios = m_genscenarios(1:nscenarios,:);
78 v_pwg = v_pwg(1:nscenarios);
79
80 delta_vw = [0, 0.5, 1];
81 t_delta_vw = [t0-2, t0, t0+2];
82
83 nWGgroupsonline = 3; % 1,2 or 3 groups, equivalent to 3, 6 or 9 WGs
84 ndelta_vw = length(delta_vw); % 0, 0.5, 1 m/s
85 nt_delta_vw = length(t_delta_vw); % 2s before, 0s, 2s after CG loss
86 ngenonline = 8; % there is at most 8 CGs per scenario
87
88 % preallocate output cells (save computation time)
89 c_t_wg = cell(nscenarios, ngenonline, nWGgroupsonline,
90     ndelta_vw, nt_delta_vw);
91 c_w_wg = cell(nscenarios, ngenonline, nWGgroupsonline,
92     ndelta_vw, nt_delta_vw);

```

```

89 c_pgentot_wg      = cell(nscenarios, ngenonline, nWGgroupsonline,
    ndelta_vw, nt_delta_vw);
90 c_pufls_wg       = cell(nscenarios, ngenonline, nWGgroupsonline,
    ndelta_vw, nt_delta_vw);
91 c_pgenWGtot_wg   = cell(nscenarios, ngenonline, nWGgroupsonline,
    ndelta_vw, nt_delta_vw);
92 c_WGpenetration_wg = cell(nscenarios, ngenonline, nWGgroupsonline,
    ndelta_vw, nt_delta_vw);
93
94 m_fmin = zeros(nscenarios, ngenonline, nWGgroupsonline, ndelta_vw,
    nt_delta_vw);
95 m_fss  = zeros(nscenarios, ngenonline, nWGgroupsonline, ndelta_vw,
    nt_delta_vw);
96 m_pufls = zeros(nscenarios, ngenonline, nWGgroupsonline, ndelta_vw,
    nt_delta_vw);
97
98 ngenscenarios = size(m_genscenarios,1);
99
100 % set fixed simulation block paramters
101 set_param([powersystemdl(1:end-4) '/UFLS'],'v_dfufpu',['[' sprintf('%f ',
    v_dfufpu) '']],...
102     'v_tintuf',['[' sprintf('%f ',v_tintuf) '']], 'v_topnuf',['[' sprintf(
    '%f ',v_topnuf) '']],...
103     'v_dfrocofpu',['[' sprintf('%f ',v_dfrocofpu) '']], 'v_dfdtrocofpu',['
    [' sprintf('%f ',v_dfdtrocofpu) '']],...
104     'v_tintrocof',['[' sprintf('%f ',v_tintrocof) '']], 'v_topnrocof',['['
    sprintf('%f ',v_topnrocof) ']]); % set UFLS parameters
105
106 set_param([powersystemdl(1:end-4) '/Perturbation'],'time',['[' sprintf('%
    f',t0) '']], 'Sampletime','0'); % set perturbation parameters
107
108 set_param(powersystemdl(1:end-4), 'StopTime',sprintf('%f',tsimulation));
109
110 % set fixed WG parameters
111 for i = 0:numWG-1
112     set_param([powersystemdl(1:end-4) '/WindGenerator' int2str(i)], 'R',
        sprintf('%f',R), 'Hw',sprintf('%f',Hw));
113 end
114
115 % simulate each scenario
116 for igenscenario = ngenscenarios:-1:1
117
118     fprintf('Scenario: %i', igenscenario);
119
120     pinitwindgen = v_pwg(igenscenario); % in MW
121
122     % initialise the WGs for each scenario
123     [vw0, wr0, pinitwindgen, ~, ~, ~, ~, ~, ~, ~] = fun_WGmodel_startup(
        powersystemdl(1:end-4), pinitwindgen, Pn, diameter); % in pu
124
125     for i = 0:numWG-1
126         set_param([powersystemdl(1:end-4) '/WindGenerator' int2str(i)], '
            pinitwindgen',sprintf('%f',pinitwindgen), 'wr0',sprintf('%f',
            wr0));
127     end
128

```

```

129 % initialise initial wind speed
130 set_param([powersystemdl(1:end-4) '/Wind'], 'Before', ['[' sprintf('%f
    ',vw0) '']]);
131
132 % get generation scenario
133 v_genscenario = m_genscenarios(igenscenario,:); % generation of each
    unit in MW
134 pdem_CG = sum(v_genscenario); % demand = sum of generation (in MW)
135
136 % get online units
137 v_igenonline = find(v_genscenario>0); % a unit is online if its
    generation > 0 MW
138 ngenonline = length(v_igenonline);
139
140 % simulate every single generator outage
141 for igenonline = 1:ngenonline
142
143     % remaining units
144     v_iremgenonline = v_igenonline;
145     v_iremgenonline(igenonline) = []; % take out the lost generator
146     ngen = length(v_iremgenonline);
147
148     % set model parameters
149     fun_setsimulinkblockparameters(powersystemdl(1:end-4),ngen,
        m_gendata, ...
150         v_genscenario,v_igenonline,igenonline,v_iremgenonline, Pn); %
        v_pshed0MW
151
152     for WGgroupsonline = 1:3
153
154         % base power to convert everything in pu on system basis
155         v_Mbase = m_gendata(4,v_iremgenonline);
156         Sbase = sum(v_Mbase);
157
158         pdem = pdem_CG + WGgroupsonline*3*pinitwindgen*Pn; % total
            demand in MW (Pn = 1.5 MW)
159         v_pshed0MW = v_pshed0/100*pdem;
160
161         v_pshed0pu = v_pshed0MW/Sbase;
162         % set UFLS parameters (step size only)
163         set_param([powersystemdl(1:end-4) '/UFLS'],'v_pshed0pu',['['
            sprintf('%f ',v_pshed0pu) '']]);
164
165         % set the right number of WGs
166         set_param([powersystemdl(1:end-4) '/numWG'],'Value',['['
            sprintf('%f',WGgroupsonline) '']]);
167
168         i_delta_vw = 1;
169
170         for delta_vw = [0, 0.5, 1]
171
172             % initialise the change in wind speed
173             set_param([powersystemdl(1:end-4) '/Wind'],'After',['['
                sprintf('%f',vw0-delta_vw) '']]);
174
175             i_t_delta_vw = 1;

```

```

176
177     for t_delta_vw = [t0-2, t0, t0+2]
178
179         % initialise the time of the wind speed change
180         set_param([powersystemdl(1:end-4) '/Wind'],'time',[
181             ' sprintf('%f',t0+t_delta_vw) ']);
182
183         % simulate it and store results
184         [c_t_wg{igensscenario, igenonline, WGgroupsonline,
185             i_delta_vw, i_t_delta_vw},~, ...
186             c_w_wg{igensscenario, igenonline, WGgroupsonline,
187                 i_delta_vw, i_t_delta_vw}, ...
188             c_pgentot_wg{igensscenario, igenonline,
189                 WGgroupsonline, i_delta_vw, i_t_delta_vw}, ...
190             c_pufls_wg{igensscenario, igenonline,
191                 WGgroupsonline, i_delta_vw, i_t_delta_vw}, ...
192             c_pgenWGtot_wg{igensscenario, igenonline,
193                 WGgroupsonline, i_delta_vw, i_t_delta_vw}, ...
194             c_WGpenetration_wg{igensscenario, igenonline,
195                 WGgroupsonline, i_delta_vw, i_t_delta_vw}] =
196             sim(powersystemdl);
197
198         % change from pu units to MWs
199         c_pgentot_wg{igensscenario, igenonline, WGgroupsonline
200             , i_delta_vw, i_t_delta_vw} = ...
201             Sbase * c_pgentot_wg{igensscenario, igenonline,
202                 WGgroupsonline, i_delta_vw, i_t_delta_vw};
203         c_pufls_wg{igensscenario, igenonline, WGgroupsonline,
204             i_delta_vw, i_t_delta_vw} = ...
205             Sbase * c_pufls_wg{igensscenario, igenonline,
206                 WGgroupsonline, i_delta_vw, i_t_delta_vw};
207         c_pgenWGtot_wg{igensscenario, igenonline,
208             WGgroupsonline, i_delta_vw, i_t_delta_vw} = ...
209             Sbase * c_pgenWGtot_wg{igensscenario, igenonline,
210                 WGgroupsonline, i_delta_vw, i_t_delta_vw};
211         c_w_wg{igensscenario, igenonline, WGgroupsonline,
212             i_delta_vw, i_t_delta_vw} = ...
213             fbase + fbase * c_w_wg{igensscenario, igenonline,
214                 WGgroupsonline, i_delta_vw, i_t_delta_vw};
215
216         % store igensscenario characteristics
217         m_fss(igensscenario, igenonline, WGgroupsonline,
218             i_delta_vw, i_t_delta_vw) = ...
219             c_w_wg{igensscenario, igenonline, WGgroupsonline,
220                 i_delta_vw, i_t_delta_vw}(end);
221         m_fmin(igensscenario, igenonline, WGgroupsonline,
222             i_delta_vw, i_t_delta_vw) = ...
223             min(c_w_wg{igensscenario, igenonline,
224                 WGgroupsonline, i_delta_vw, i_t_delta_vw});
225         m_pufls(igensscenario, igenonline, WGgroupsonline,
226             i_delta_vw, i_t_delta_vw) = ...
227             c_pufls_wg{igensscenario, igenonline,
228                 WGgroupsonline, i_delta_vw, i_t_delta_vw}(end)
229             ;
230
231     end
232
233
234
235
236
237
238

```

```

209         i_t_delta_vw = i_t_delta_vw + 1;
210     end
211     i_delta_vw = i_delta_vw + 1;
212 end
213     end
214 end
215 end
216
217 disp('Simulation stops.');
```

---

```

218
219 % close_system(powersystemmdl,0);
220
221 %%
222 -----
223
222 % Display frequency deviation (among other things) for different
223 % parameters
224 -----
225
224 v_colours = ["#EDB120" "#7E2F8E" "#77AC30" "#4DBEEE" "#A2142F" "#AE43F0"
225             "#0076A8" "#0072BD" "#D95319"];
226
227 % ==> Choose parameters to print out their simulation here
228 igenscenario = 1; % scenario 1, 2, ... 24
229 igenonline = 5; % bus number being disconnected
230 WGgroupsonline = 3; % 1, 2, 3 WGs groups (so 3, 6, 9 WGs)
231 i_delta_vw = 1; % 0, 0.5, 1 m/s
232 i_t_delta_vw = 2; % 2s before, 0s, 2s after
233 nscenarios = 1; % 1, 2, ... 24
234
235
236 %%
237 % use matlab2tikz('scenario1_nodroop.tex','width','\figW','height','\figH
238 % to translate matlab figures to tikz
239
240 fun_graphScenarios(igenonline, WGgroupsonline, i_t_delta_vw, i_delta_vw,
241                   nscenarios, c_t_wg, c_w_wg, c_pufls_wg, c_WGpenetration_wg,
242                   c_pgenWGtot_wg, c_pgentot_wg, v_colours, m_fss, m_fmin, m_pufls)
243
244 fun_graphGeneratorLoss(igenscenario, WGgroupsonline, i_t_delta_vw,
245                        i_delta_vw, m_igen scenarios, c_t_wg, c_w_wg, c_pufls_wg,
246                        c_WGpenetration_wg, c_pgenWGtot_wg, c_pgentot_wg, v_colours, m_fss,
247                        m_fmin, m_pufls)
248
249 fun_graphWGs(igenscenario, igenonline, i_delta_vw, i_t_delta_vw, c_t_wg,
250             c_w_wg, c_pufls_wg, c_WGpenetration_wg, c_pgenWGtot_wg, c_pgentot_wg,
251             v_colours, m_fss, m_fmin, m_pufls)
252
253 fun_graphWindSpeed(igenscenario, igenonline, WGgroupsonline, i_t_delta_vw,
254                   c_t_wg, c_w_wg, c_pufls_wg, c_WGpenetration_wg, c_pgenWGtot_wg,
255                   c_pgentot_wg, v_colours, m_fss, m_fmin, m_pufls)
256
257
258
259
260
261
262
263
264
265
266
267
268
269
270
271
272
273
274
275
276
277
278
279
280
281
282
283
284
285
286
287
288
289
290
291
292
293
294
295
296
297
298
299
300
301
302
303
304
305
306
307
308
309
310
311
312
313
314
315
316
317
318
319
320
321
322
323
324
325
326
327
328
329
330
331
332
333
334
335
336
337
338
339
340
341
342
343
344
345
346
347
348
349
350
351
352
353
354
355
356
357
358
359
360
361
362
363
364
365
366
367
368
369
370
371
372
373
374
375
376
377
378
379
380
381
382
383
384
385
386
387
388
389
390
391
392
393
394
395
396
397
398
399
400
401
402
403
404
405
406
407
408
409
410
411
412
413
414
415
416
417
418
419
420
421
422
423
424
425
426
427
428
429
430
431
432
433
434
435
436
437
438
439
440
441
442
443
444
445
446
447
448
449
450
451
452
453
454
455
456
457
458
459
460
461
462
463
464
465
466
467
468
469
470
471
472
473
474
475
476
477
478
479
480
481
482
483
484
485
486
487
488
489
490
491
492
493
494
495
496
497
498
499
500

```

```

248 fun_graphWindTiming(igenscenario, igenonline, WGgroupsonline, i_delta_vw,
    c_t_wg, c_w_wg, c_pufls_wg, c_WGpenetration_wg, c_pgenWGtot_wg,
    c_pgentot_wg, v_colours, m_fss, m_fmin, m_pufls)
249
250 [v_sum_pufls_delta_vw, v_sum_delta_fmin_delta_vw, v_sum_pufls_t_delta_vw,
    v_sum_delta_fmin_t_delta_vw] = ...
251     fun_sums(m_pufls, m_fmin, fbase, ngenscenarios, m_igenscenarios, t0);
252
253 fun_sim_no_droop(powersystemmdl, igenscenario, igenonline, WGgroupsonline,
    i_delta_vw, i_t_delta_vw, ...
254     c_t_wg, c_w_wg, c_pufls_wg, c_WGpenetration_wg, c_pgenWGtot_wg,
    c_pgentot_wg, t0, numWG, m_igenscenarios, m_gendata, v_pshed0, v_pwg
    , Pn, diameter, fbase);
255
256 toc

```

### 6.2.2 Power-speed curve

```

1 function [m_pw,v_wr,v_pwmpp,v_wrmpp,v_pwdel,v_wrdel, vw0, wr0,
    pinitwindgen] = fun_getwindpowercurve(v_beta,v_vw, pinitwindgenMW, Pn,
    diameter)
2
3 % This function computes the power-speed curves (MPP and deloaded
    operation
4 % modes) for wind generation.
5 % The power-speed curve of a wind generator is used for this
6 % purpose. The resulting curve must be appropriately scaled.
7 %
8 % Input:    angle of attack (beta), wind speed (v_vw), initial Power
9 %           (pinitwindgen), nominal P (Pn), rotor diameter
10 % Output:  wind power, pw; rotor speed, wr; MPP power, pwmpp; MPP rotor
11 %           speed, wrmpp; deloaded power, pwdel; deloaded rotor speed,
12 %           wrdel
13
14 deload = 0.1;    % percentage of deloading
15 rho = 1.275;    % air density
16
17 v_Wr = 0:0.01:3.4; % rotor speed range (rad/s)
18
19 Pn = Pn * 1e6;
20 Rb = diameter/2; % blade radius (m)
21
22 v_cp = [0.73, 151, 0.58, 0.002, 2.14, 13.2, 18.4, -0.02, -0.003]; %
    performance coefficients
23
24 Aw = Rb^2*pi; % surface
25
26 pinitwindgen = pinitwindgenMW/(Pn * 1e-6);
27
28 nvw = length(v_vw);
29 nwr = length(v_Wr);
30
31 m_pw    = zeros(nvw,nwr);
32 v_wr    = zeros(1,nwr);
33 v_pwmpp = zeros(nvw,1);

```

```

34 v_wrmpp = zeros(1,nvw);
35 v_pwdel = zeros(nvw,1);
36 v_wrdel = zeros(1,nvw);
37 v_iwrmpp= zeros(nvw,1);
38
39 for iw = nvw:-1:1 % for every wind speed:
40
41     vw = v_vw(iw);
42     lambda = v_Wr*Rb./vw;
43     delta = (1./(lambda+v_cp(8).*v_beta)-v_cp(9)./(1+v_beta.^3));
44     Cp = v_cp(1)*(v_cp(2).*delta-v_cp(3).*v_beta-v_cp(4).*v_beta.^v_cp(5)
45         -v_cp(6)).*exp(-v_cp(7).*delta);
46     m_pw(iw,:) = Cp*rho/2*Aw*vw.^3/Pn; % per unit mechanical power
47
48 end
49 [v_pwmpp,v_iwrmpp] = max(m_pw,[],2); % MPP
50 v_pwdel = (1-deload) * v_pwmpp; % deloaded
51
52 v_iwrdel= zeros(1,nvw);
53 v_wrdel = zeros(1,nvw+5);
54 v_Wrdel = zeros(1,nvw+5);
55
56 % find closest deloaded value that corresponds to pinitwindgen
57 i_pinitwindgen_lower = find(v_pwdel <= pinitwindgen,1,'last');
58 i_pinitwindgen_higher = find(v_pwdel >= pinitwindgen,1,'first');
59
60 % interpolate to find initial wind speed
61 vw0 = v_vw(i_pinitwindgen_lower) + ...
62     (v_vw(i_pinitwindgen_higher)-v_vw(i_pinitwindgen_lower))*(
63     pinitwindgen-v_pwdel(i_pinitwindgen_lower))/(v_pwdel(
64     i_pinitwindgen_higher)-v_pwdel(i_pinitwindgen_lower));
65
66 for iw = nvw:-1:1
67     % it takes the right half of the curve after the MPP point
68     % corresponding to that
69     % particular wind speed
70
71     [~,v_iwrdel(iw)] = min(abs(m_pw(iw,v_iwrmpp(iw):end) - v_pwdel(iw)));
72     v_Wrdel(iw) = v_Wr(v_iwrmpp(iw)+v_iwrdel(iw)); % gives the
73     % corresponding wr
74
75 end
76
77 % find closest rotor speed value that corresponds to Wr0
78 Wr0_lower = v_Wrdel(i_pinitwindgen_lower);
79 Wr0_higher = v_Wrdel(i_pinitwindgen_higher);
80
81 % interpolate
82 Wr0 = Wr0_lower + ...
83     (Wr0_higher-Wr0_lower)*(pinitwindgen-v_pwdel(i_pinitwindgen_lower))/(
84     v_pwdel(i_pinitwindgen_higher)-v_pwdel(i_pinitwindgen_lower));
85
86 % we add a few "deloaded" points so that, when the wind speed becomes
87 % higher
88 % than the maximum specified one, the maximum power has been reached
89 for i_extra_vw = 1:5

```

```

83     v_pwdel(nvw+i_extra_vw) = v_pwdel(nvw);
84     v_Wrdel(nvw+i_extra_vw) = v_Wrdel(nvw) + i_extra_vw * (v_Wr(length(
        v_Wr))-v_Wrdel(nvw))/5;
85 end
86
87 ipwmppn = find(v_pwmpp<=1,1,'last');    % nominal power (1 pu)
88 Wrn = v_Wr(v_iwrmpn(ipwmppn));        % nominal speed
89 v_wr = v_Wr/Wrn;
90
91 v_Wrmpn = v_Wr(v_iwrmpn);
92 v_wrmpn = v_Wrmpn/Wrn; % speed corresponding to MPP
93 v_wrdel = v_Wrdel/Wrn; % speed corresponding to deloaded operation
    points
94
95 wr0      = Wr0/Wrn;    % turning to pu
96
97 %% TO DRAW FIGURE WR-PW CURVE:
98 figure;
99 title('MPP and Deloaded operation')
100 % plot(v_wr,m_pw','b');hold on;
101 plot(v_wrmpn,v_pwmpp,'-r');hold on;
102 plot(v_wrdel,v_pwdel,'-b');hold on;
103 legend('MPP','Deloaded')
104 plot(wr0,pinitwindgen,'*', 'linewidth',4,'HandleVisibility','off');hold
    on;
105
106 plot(v_wr,m_pw','b', 'HandleVisibility','off');hold on;
107 xlabel('Rotor speed (pu)')
108 ylabel('Mechanical power (pu)')
109 hold off;
110 sgt = sgtitle('Power-speed curve', 'interpreter','latex');
111 sgt.FontSize = 18;

```

### 6.2.3 Setting Simulink parameters

```

1 function fun_setsimulinkblockparameters(powersystemdl,ngen,m_gendata, ...
2     v_genscenario,v_igenonline,igenonline,v_iremgenonline, Pn) %
    v_pshedOMW
3
4 % Prepares and sets the parameters of the blocks of the Simulink model.
5
6 v_pinit = v_genscenario(v_iremgenonline); % the initial power for the
7
8 % base power to convert everything in pu on system basis
9 v_Mbase = m_gendata(4,v_iremgenonline);
10 Sbase = sum(v_Mbase);
11
12 % calculate the total generated power by CG
13 pgenCGtot = 0;
14 for i=1:ngen+1 % iterate through ALL generators
15     pgenCGtot = pgenCGtot + v_genscenario(v_igenonline(i)); % sum the
        power (in MW) of the all the CGs in the scenario
16 end
17 pgenCGtot = pgenCGtot/Sbase; % to make it in pu
18

```



```

19 % lost amount of power
20 plostopu = v_genscenario(v_igenonline(igenonline))/Sbase;
21
22 % get dynamic parameters of remaining units
23 v_h = m_gendata(3,v_iremgenonline); % pu on generator rating basis
24 heq = v_h*v_Mbase(:)/Sbase;
25 close all
26
27 v_kpugenrating = m_gendata(2,v_iremgenonline); % pu on generator rating
    basis
28 v_kgpu = v_kpugenrating.*v_Mbase/Sbase;
29
30 v_bg1 = m_gendata(7,v_iremgenonline);
31 v_bg2 = m_gendata(8,v_iremgenonline);
32 v_ag1 = m_gendata(9,v_iremgenonline);
33 v_ag2 = m_gendata(10,v_iremgenonline);
34
35 [m_Ag,m_Bg,m_Cg,m_Dg] = fun_getstatespace(nngen,v_kgpu,v_bg1,v_bg2,v_ag1,
    v_ag2);
36 v_dpgmaxpu = (m_gendata(5,v_iremgenonline)-v_pinit)/Sbase;
37 v_dpgminpu = (m_gendata(6,v_iremgenonline)-v_pinit)/Sbase;
38
39 % set rotor parameters
40 set_param([powersystemdl '/Rotor'],'Numerator', '[0 1]','Denominator', ['
    [2*', sprintf('%f',heq), ' 0]']);
41
42 % set generator state space parameters
43 set_param([powersystemdl '/State-Space-Gen'],'A',mat2str(m_Ag),'B',
    mat2str(m_Bg),'C',mat2str(m_Cg),'D',mat2str(m_Dg));
44
45 % set generator power limits
46 set_param([powersystemdl '/Powerlimits'],'UpperLimit',['[ sprintf('%f ',
    v_dpgmaxpu) ']'],'LowerLimit',['[ sprintf('%f ',v_dpgminpu) ']']);
47
48 % set perturbation parameters (plostopu only)
49 set_param([powersystemdl '/Perturbation'],'After',['[ sprintf('%f',
    plostopu) ']'],'Before','0');
50
51 % WG-RELATED PARAMETERS
52 % set system base change parameters (System base only, where the system
    base is the sum of the Mbase's of the CG)
53 set_param([powersystemdl '/SystemBaseChange'],'Gain',['[ sprintf('%f',Pn
    ) '/' sprintf('%f',Sbase) ']']);
54
55 % set system base change parameters (System base only, where the system
    base is the sum of the Mbase's of the CG)
56 set_param([powersystemdl '/SystemBaseChange1'],'Gain',['[ sprintf('%f',
    Pn) '/' sprintf('%f',Sbase) ']']);
57
58 % set total generated power by the CG (the actual one; not the change in
59 % power generation)
60 set_param([powersystemdl '/pgenCGtot'],'Value',['[ sprintf('%f ',
    pgenCGtot) ']']);

```

### 6.2.4 Plotting and printing data

Only one of the visualiser functions is shown here, simply because the other ones are quite similar.

```

1 function fun_graphGeneratorLoss(igenscenario, WGgroupsonline,
  i_t_delta_vw, i_delta_vw, ...
2     m_genscenarios, c_t_wg, c_w_wg, c_pufls_wg, c_WGpenetration_wg,
  c_pgenWGtot_wg, c_pgentot_wg, ...
3     v_colours, m_fss, m_fmin, m_pufls)
4
5 % This function shows several signals (including the frequency) with
6 % different Gens shutting off
7
8 ngenonline = length(find(m_genscenarios(igenscenario,:)>0)); % a unit is
  online if its generation > 0 MW
9
10 hf = figure('WindowState','maximized');
11 subplot(5,1,1);
12
13 % labels = cellstr(num2str((1:ngenonline)'));
14 labels = cellstr(num2str((1:ngenonline)', 'Gen. %d'));
15
16 for igenonline = 1:ngenonline
17     plot(c_t_wg{igenscenario, igenonline, WGgroupsonline, i_delta_vw,
  i_t_delta_vw}, ...
18         c_w_wg{igenscenario, igenonline, WGgroupsonline, i_delta_vw,
  i_t_delta_vw}, ...
19         'Color',v_colours(igenonline));hold on;
20 end
21 legend(labels);
22 ylabel('Freq \omega (Hz)')
23 ylim('padded')
24 hold off;
25
26 subplot(5, 1, 2);
27
28 for igenonline = 1:ngenonline
29     plot(c_t_wg{igenscenario, igenonline, WGgroupsonline, i_delta_vw,
  i_t_delta_vw}, ...
30         c_pufls_wg{igenscenario, igenonline, WGgroupsonline, i_delta_vw,
  i_t_delta_vw}, ...
31         'Color',v_colours(igenonline));hold on;
32 end
33 ylabel('P_{shed}^{UFLS} (MW)')
34 ylim('padded')
35 hold off;
36
37 subplot(5, 1, 3);
38
39 for igenonline = 1:ngenonline
40     plot(c_t_wg{igenscenario, igenonline, WGgroupsonline, i_delta_vw,
  i_t_delta_vw}, ...
41         c_WGpenetration_wg{igenscenario, igenonline, WGgroupsonline,
  i_delta_vw, i_t_delta_vw}, ...
42         'Color',v_colours(igenonline));hold on;
43 end
44 ylabel('WG pen. (%)')

```

```

45 ylim('padded')
46 hold off;
47
48 subplot(5, 1, 4);
49
50 for igenonline = 1:ngenonline
51     plot(c_t_wg{igenscenario, igenonline, WGgroupsonline, i_delta_vw,
52         i_t_delta_vw}, ...
53         c_pgenWGtot_wg{igenscenario, igenonline, WGgroupsonline,
54             i_delta_vw, i_t_delta_vw}, ...
55         'Color',v_colours(igenonline));hold on;
56 end
57 ylabel('P_{gen}^{WG} (MW)')
58 ylim('padded')
59 hold off;
60
61 subplot(5, 1, 5);
62
63 for igenonline = 1:ngenonline
64     plot(c_t_wg{igenscenario, igenonline, WGgroupsonline, i_delta_vw,
65         i_t_delta_vw}, ...
66         c_pgentot_wg{igenscenario, igenonline, WGgroupsonline, i_delta_vw,
67             i_t_delta_vw}, ...
68         'Color',v_colours(igenonline));hold on;
69 end
70 xlabel('Time (s)')
71 ylabel('P_{gen}^{tot} (MW)')
72 ylim('padded')
73 hold off;
74
75 sgt = sgttitle(['Scenario ', num2str(igenscenario)], 'Color', "#0072BD", '
76     interpreter', 'latex');
77 sgt.FontSize = 18;
78
79 %% LaTeX table
80
81 % Initialize LaTeX table
82 latexTable = sprintf('\begin{table}[ht]\n');
83 latexTable = [latexTable, sprintf('    \centering\n)];
84 latexTable = [latexTable, sprintf('    \caption{Indices.}\n)];
85 latexTable = [latexTable, sprintf('    \begin{tabular}{cccc}\n)];
86 latexTable = [latexTable, sprintf('    \\\n)];
87
88 % Add table header
89 latexTable = [latexTable, sprintf('    %s & %s & %s & %s \\\n', 'Lost
90     CG', '$f_{ss}$ (Hz)$', '$f_{min}$ (Hz)$', '$P_{ufls}$ (MW)$)];
91 latexTable = [latexTable, sprintf('    \\\hline\n)];
92
93 % Add table content
94 for igenonline = 1:ngenonline
95     latexTable = [latexTable, sprintf('    %d & %.4f & %.4f & %.4f \\\n
96         ', igenonline, ...
97         m_fss(igenscenario, igenonline, WGgroupsonline, i_delta_vw,
98             i_t_delta_vw), ...
99         m_fmin(igenscenario, igenonline, WGgroupsonline, i_delta_vw,
100             i_t_delta_vw), ...

```

```

92         m_pufls(igenscenario, igenonline, WGgroupsonline, i_delta_vw,
93             i_t_delta_vw));
94     end
95     % Finalize LaTeX table
96     latexTable = [latexTable, sprintf('    \\hline\n')];
97     latexTable = [latexTable, sprintf('    \\end{tabular}\n')];
98     latexTable = [latexTable, sprintf('    \\label{tb:results}\n')];
99     latexTable = [latexTable, sprintf('\\end{table}')];
100
101     % Print the LaTeX table
102     disp(latexTable);

```

### 6.2.5 Obtaining the sum of the frequency deviations and load shed of all simulations for the each parameter

This function is of great relevance to see the effect each parameter has on the system stability. It would be more optimal to integrate it into the existing loops within the *main\_rundynamicsimulation* main file, however this function is meant to be used on its own once the workspace with the simulation data has been saved.

```

1  function [v_sum_pufls_delta_vw, v_sum_delta_fmin_delta_vw,
2      v_sum_pufls_t_delta_vw, v_sum_delta_fmin_t_delta_vw] = ...
3      fun_sums(m_pufls, m_fmin, fbase, ngenscenarios, m_ongenscenarios, t0)
4
5  v_sum_pufls_delta_vw      = zeros(1,3);
6  v_sum_delta_fmin_delta_vw = zeros(1,3);
7  v_sum_pufls_t_delta_vw   = zeros(1,3);
8  v_sum_delta_fmin_t_delta_vw = zeros(1,3);
9  v_sum_pufls_WGgroups      = zeros(1,3);
10 v_sum_delta_fmin_WGgroups = zeros(1,3);
11
12 for igenscenario = ngenscenarios:-1:1
13     % get generation scenario
14     v_ongenscenario = m_ongenscenarios(igenscenario,:); % generation of each
15     % unit in MW
16     % get online units
17     v_igenonline = find(v_ongenscenario>0); % a unit is online if its
18     % generation > 0 MW
19     ngenonline = length(v_igenonline);
20
21     for igenonline = 1:ngenonline
22         for WGgroupsonline = 1:3
23             i_delta_vw = 1;
24             for delta_vw = [0, 0.5, 1]
25                 i_t_delta_vw = 1;
26                 for t_delta_vw = [t0-2, t0, t0+2]
27
28                     if WGgroupsonline == 1
29                         v_sum_pufls_WGgroups(1) =
30                             v_sum_pufls_WGgroups(1) + m_pufls(
31                                 igenscenario, igenonline, WGgroupsonline,
32                                 i_delta_vw, i_t_delta_vw);
33                         v_sum_delta_fmin_WGgroups(1) =
34                             v_sum_delta_fmin_WGgroups(1) + fbase - m_fmin(

```

```

        igenscenario, igenonline, WGgroupsonline,
        i_delta_vw, i_t_delta_vw);
29 elseif WGgroupsonline == 2
30     v_sum_pufls_WGgroups(2) =
        v_sum_pufls_WGgroups(2) + m_pufls(igenscenario
        , igenonline, WGgroupsonline, i_delta_vw,
        i_t_delta_vw);
31     v_sum_delta_fmin_WGgroups(2) =
        v_sum_delta_fmin_WGgroups(2) + fbase - m_fmin(
        igenscenario, igenonline, WGgroupsonline,
        i_delta_vw, i_t_delta_vw);
32 elseif WGgroupsonline == 3
33     v_sum_pufls_WGgroups(3) =
        v_sum_pufls_WGgroups(3) + m_pufls(igenscenario
        , igenonline, WGgroupsonline, i_delta_vw,
        i_t_delta_vw);
34     v_sum_delta_fmin_WGgroups(3) =
        v_sum_delta_fmin_WGgroups(3) + fbase - m_fmin(
        igenscenario, igenonline, WGgroupsonline,
        i_delta_vw, i_t_delta_vw);
35 end
36
37 if delta_vw == 0
38     v_sum_pufls_delta_vw(1) =
        v_sum_pufls_delta_vw(1) + m_pufls(
        igenscenario, igenonline, WGgroupsonline,
        i_delta_vw, i_t_delta_vw);
39     v_sum_delta_fmin_delta_vw(1) =
        v_sum_delta_fmin_delta_vw(1) + fbase - m_fmin(
        igenscenario, igenonline, WGgroupsonline,
        i_delta_vw, i_t_delta_vw);
40 elseif delta_vw == 0.5
41     v_sum_pufls_delta_vw(2) =
        v_sum_pufls_delta_vw(2) + m_pufls(igenscenario
        , igenonline, WGgroupsonline, i_delta_vw,
        i_t_delta_vw);
42     v_sum_delta_fmin_delta_vw(2) =
        v_sum_delta_fmin_delta_vw(2) + fbase - m_fmin(
        igenscenario, igenonline, WGgroupsonline,
        i_delta_vw, i_t_delta_vw);
43 elseif delta_vw == 1
44     v_sum_pufls_delta_vw(3) =
        v_sum_pufls_delta_vw(3) + m_pufls(igenscenario
        , igenonline, WGgroupsonline, i_delta_vw,
        i_t_delta_vw);
45     v_sum_delta_fmin_delta_vw(3) =
        v_sum_delta_fmin_delta_vw(3) + fbase - m_fmin(
        igenscenario, igenonline, WGgroupsonline,
        i_delta_vw, i_t_delta_vw);
46 end
47
48 if t_delta_vw == t0-2
49     v_sum_pufls_t_delta_vw(1) =
        v_sum_pufls_t_delta_vw(1) + m_pufls(
        igenscenario, igenonline, WGgroupsonline,
        i_delta_vw, i_t_delta_vw);

```

```

50         v_sum_delta_fmin_t_delta_vw(1) =
           v_sum_delta_fmin_t_delta_vw(1) + fbase -
           m_fmin(igenscenario, igenonline,
           WGgroupsonline, i_delta_vw, i_t_delta_vw);
51     elseif t_delta_vw == t0
52         v_sum_pufls_t_delta_vw(2) =
           v_sum_pufls_t_delta_vw(2) + m_pufls(
           igenscenario, igenonline, WGgroupsonline,
           i_delta_vw, i_t_delta_vw);
53         v_sum_delta_fmin_t_delta_vw(2) =
           v_sum_delta_fmin_t_delta_vw(2) + fbase -
           m_fmin(igenscenario, igenonline,
           WGgroupsonline, i_delta_vw, i_t_delta_vw);
54     elseif t_delta_vw == t0+2
55         v_sum_pufls_t_delta_vw(3) =
           v_sum_pufls_t_delta_vw(3) + m_pufls(
           igenscenario, igenonline, WGgroupsonline,
           i_delta_vw, i_t_delta_vw);
56         v_sum_delta_fmin_t_delta_vw(3) =
           v_sum_delta_fmin_t_delta_vw(3) + fbase -
           m_fmin(igenscenario, igenonline,
           WGgroupsonline, i_delta_vw, i_t_delta_vw);
57     end
58
59         i_t_delta_vw = i_t_delta_vw + 1;
60     end
61     i_delta_vw = i_delta_vw + 1;
62 end
63 end
64 end
65 end
66
67 %%
68
69 latexTable = sprintf('\begin{table}[ht]\n');
70 latexTable = [latexTable, sprintf('    \centering\n')];
71 latexTable = [latexTable, sprintf('    \caption{Sums of the shed power
           and maximum deviations from the base frequency from all simulations,
           depending on the wind speed change.}\n')];
72 latexTable = [latexTable, sprintf('    \begin{tabular}{cccc}\n')];
73 latexTable = [latexTable, sprintf('        \\\n')];
74 latexTable = [latexTable, sprintf('        \\\hline\n')];
75 latexTable = [latexTable, sprintf('        %s & %s & %s & %s \\\n', ' ', '0
           $m/s$', '0.5 $m/s$', '1 $m/s$')];
76 latexTable = [latexTable, sprintf('        %s & %.1f & %.1f & %.1f \\\n', '
           $\Sigma P_{\text{ufls}}$', v_sum_pufls_delta_vw(1), v_sum_pufls_delta_vw(2),
           v_sum_pufls_delta_vw(3))];
77 latexTable = [latexTable, sprintf('        %s & %.1f & %.1f & %.1f \\\n', '
           $\Sigma \Delta f_{\text{min}}$', v_sum_delta_fmin_delta_vw(1),
           v_sum_delta_fmin_delta_vw(2), v_sum_delta_fmin_delta_vw(3))];
78 latexTable = [latexTable, sprintf('        \\\hline\n')];
79 latexTable = [latexTable, sprintf('    \end{tabular}\n')];
80 latexTable = [latexTable, sprintf('    \label{tb:sums_delta_vw}\n')];
81 latexTable = [latexTable, sprintf('\end{table}')];
82
83 % Print the LaTeX table

```

```

84 disp(latexTable);
85
86 latexTable = sprintf('\begin{table}[ht]\n');
87 latexTable = [latexTable, sprintf(' \centering\n')];
88 latexTable = [latexTable, sprintf(' \caption{Sums of the shed power
and maximum deviations from the base frequency from all simulations,
depending on the time of the wind speed change.}\n')];
89 latexTable = [latexTable, sprintf(' \begin{tabular}{cccc}\n')];
90 latexTable = [latexTable, sprintf(' \\\n')];
91 latexTable = [latexTable, sprintf(' \\\hline\n')];
92 latexTable = [latexTable, sprintf(' %s & %s & %s & %s \\\n', ' ', '
-2 $$s$', '0 $$s$', '+2 $$s$')];
93 latexTable = [latexTable, sprintf(' %s & %.1f & %.1f & %.1f \\\n', '
$\Sigma P_{ufls}$', v_sum_pufls_t_delta_vw(1), v_sum_pufls_t_delta_vw
(2), v_sum_pufls_t_delta_vw(3))];
94 latexTable = [latexTable, sprintf(' %s & %.1f & %.1f & %.1f \\\n', '
$\Sigma \Delta f_{min}$', v_sum_delta_fmin_t_delta_vw(1),
v_sum_delta_fmin_t_delta_vw(2), v_sum_delta_fmin_t_delta_vw(3))];
95 latexTable = [latexTable, sprintf(' \\\hline\n')];
96 latexTable = [latexTable, sprintf(' \end{tabular}\n')];
97 latexTable = [latexTable, sprintf(' \label{tb:sums_t_delta_vw}\n')];
98 latexTable = [latexTable, sprintf('\end{table}')];
99
100 % Print the LaTeX table
101 disp(latexTable);
102
103 latexTable = sprintf('\begin{table}[ht]\n');
104 latexTable = [latexTable, sprintf(' \centering\n')];
105 latexTable = [latexTable, sprintf(' \caption{Sums of the shed power
and maximum deviations from the base frequency from all simulations,
depending on number of WGs in the system.}\n')];
106 latexTable = [latexTable, sprintf(' \begin{tabular}{cccc}\n')];
107 latexTable = [latexTable, sprintf(' \\\n')];
108 latexTable = [latexTable, sprintf(' \\\hline\n')];
109 latexTable = [latexTable, sprintf(' %s & %s & %s & %s \\\n', ' ', '3
WGs', '6 WGs', '9 WGs')];
110 latexTable = [latexTable, sprintf(' %s & %.1f & %.1f & %.1f \\\n', '
$\Sigma P_{ufls}$', v_sum_pufls_WGgroups(1), v_sum_pufls_WGgroups(2),
v_sum_pufls_WGgroups(3))];
111 latexTable = [latexTable, sprintf(' %s & %.1f & %.1f & %.1f \\\n', '
$\Sigma \Delta f_{min}$', v_sum_delta_fmin_WGgroups(1),
v_sum_delta_fmin_WGgroups(2), v_sum_delta_fmin_WGgroups(3))];
112 latexTable = [latexTable, sprintf(' \\\hline\n')];
113 latexTable = [latexTable, sprintf(' \end{tabular}\n')];
114 latexTable = [latexTable, sprintf(' \label{tb:sums_WGs}\n')];
115 latexTable = [latexTable, sprintf('\end{table}')];
116
117 % Print the LaTeX table
118 disp(latexTable);

```

# Bibliography

- [1] P. Kundur et al. “Definition and classification of power system stability IEEE/CIGRE joint task force on stability terms and definitions”. In: *IEEE Transactions on Power Systems* 19.3 (2004), pp. 1387–1401. DOI: [10.1109/TPWRS.2004.825981](https://doi.org/10.1109/TPWRS.2004.825981).
- [2] L. Sigrist et al. *Island Power Systems*. CRC Press, Taylor & Francis Group, 2016. ISBN: 9781498746380.
- [3] IRENA. *Renewable Capacity Statistics 2022*. Último acceso: 29-06-2023. IRENA, 2022, p. 14. ISBN: 978-92-9260-428-8. URL: <https://www.irena.org/publications/2022/Apr/Renewable-Capacity-Statistics-2022>.
- [4] United Nations. *Sustainable Development Goal 7*. Accessed: 05/06/2023. United Nations. 2023. URL: <https://sdgs.un.org/goals/goal7>.
- [5] Abdul W. Korai et al. “Generic DSL-Based Modeling and Control of Wind Turbine Type 4 for EMT Simulations in DIgSILENT PowerFactory”. In: *Advanced Smart Grid Functionalities Based on PowerFactory*. Ed. by Francisco Gonzalez-Longatt and José Luis Rueda Torres. Cham: Springer International Publishing, 2018, pp. 355–371. ISBN: 978-3-319-50532-9. DOI: [10.1007/978-3-319-50532-9\\_14](https://doi.org/10.1007/978-3-319-50532-9_14). URL: [https://doi.org/10.1007/978-3-319-50532-9\\_14](https://doi.org/10.1007/978-3-319-50532-9_14).
- [6] J.G. Slootweg et al. “General model for representing variable speed wind turbines in power system dynamics simulations”. In: *IEEE Transactions on Power Systems* 18.1 (2003), pp. 144–151. DOI: [10.1109/TPWRS.2002.807113](https://doi.org/10.1109/TPWRS.2002.807113).
- [7] Kara Clark, Nicholas W. Miller, and Juan J. Sanchez-Gasca. *Modeling of GE Wind Turbine-Generators for Grid Studies*. Tech. rep. Version 4.5. One River Road, Schenectady, NY 12345, USA: General Electric International, Inc., Apr. 2010. URL: [https://www.researchgate.net/publication/267218696\\_Modeling\\_of\\_GE\\_Wind\\_Turbine-Generators\\_for\\_Grid\\_Studies\\_Prepared\\_by](https://www.researchgate.net/publication/267218696_Modeling_of_GE_Wind_Turbine-Generators_for_Grid_Studies_Prepared_by).
- [8] James F. Conroy and Rick Watson. “Frequency Response Capability of Full Converter Wind Turbine Generators in Comparison to Conventional Generation”. In: *IEEE Transactions on Power Systems* 23.2 (2008), pp. 649–656. DOI: [10.1109/TPWRS.2008.920197](https://doi.org/10.1109/TPWRS.2008.920197).
- [9] O. Wasynczuk, D. T. Man, and J. P. Sullivan. “Dynamic Behavior of a Class of Wind Turbine Generators During Random Wind Fluctuations”. In: *IEEE Transactions on Power Apparatus and Systems* PAS-100.6 (1981), pp. 2837–2845. DOI: [10.1109/TPAS.1981.316400](https://doi.org/10.1109/TPAS.1981.316400).
- [10] O. Apata and D.T.O. Oyedokun. “An overview of control techniques for wind turbine systems”. In: *Scientific African* 10 (2020), e00566. ISSN: 2468-2276. DOI: <https://doi.org/10.1016/j.sciaf.2020.e00566>. URL: <https://www.sciencedirect.com/science/article/pii/S2468227620303045>.
- [11] Hongtao ma and Badrul Chowdhury. “Working towards frequency regulation with wind plants: Combined control approaches”. In: *Renewable Power Generation, IET* 4 (Aug. 2010), pp. 308–316. DOI: [10.1049/iet-rpg.2009.0100](https://doi.org/10.1049/iet-rpg.2009.0100).
- [12] Chittaranjan Pradhan and Chandrashekhara Bhende. “Enhancement in Primary Frequency Contribution using Dynamic Deloading of Wind Turbines”. In: *IFAC-PapersOnLine* 48.30 (2015). 9th IFAC Symposium on Control of Power and Energy Systems CPES 2015, pp. 13–18. ISSN: 2405-8963. DOI: <https://doi.org/10.1016/j.ifacol.2015.12.346>. URL: <https://www.sciencedirect.com/science/article/pii/S2405896315029882>.



- [13] James Boyle et al. “An alternative frequency-droop scheme for wind turbines that provide primary frequency regulation via rotor speed control”. In: *International Journal of Electrical Power & Energy Systems* 133 (2021), p. 107219. ISSN: 0142-0615. DOI: <https://doi.org/10.1016/j.ijepes.2021.107219>. URL: <https://www.sciencedirect.com/science/article/pii/S0142061521004580>.
- [14] K. V. Vidyanandan and Nilanjan Senroy. “Primary frequency regulation by deloaded wind turbines using variable droop”. In: *IEEE Transactions on Power Systems* 28 (2013), pp. 837–846.
- [15] Ministerio de Industria, Turismo y Comercio. “Resolución de 28 de abril de 2006, de la Secretaría General de Energía, por la que se aprueba un conjunto de procedimientos de carácter técnico e instrumental necesarios para realizar la adecuada gestión técnica de los sistemas eléctricos insulares y extrapeninsulares”. In: *Boletín Oficial del Estado* 129.31 (2006), pp. 1–168.
- [16] Jan Van de Vyver et al. “Comparison of wind turbine power control strategies to provide power reserves”. In: *2016 IEEE International Energy Conference (ENERGYCON)*. IEEE, Leuven, Belgium: IEEE, Apr. 2016. DOI: [10.1109/ENERGYCON.2016.7514034](https://doi.org/10.1109/ENERGYCON.2016.7514034).
- [17] Yu-Qing Bao and Yang Li. “On deloading control strategies of wind generators for system frequency regulation”. In: *International Transactions on Electrical Energy Systems* 25.4 (2015), pp. 623–635. DOI: <https://doi.org/10.1002/etep.1855>. eprint: <https://onlinelibrary.wiley.com/doi/pdf/10.1002/etep.1855>. URL: <https://onlinelibrary.wiley.com/doi/abs/10.1002/etep.1855>.
- [18] Mohammad Rajabdorri et al. “Viability of providing spinning reserves by RES in Spanish island power systems”. In: *IET Renewable Power Generation* 15.13 (2021), pp. 2878–2890. DOI: <https://doi.org/10.1049/rpg2.12216>. eprint: <https://ietresearch.onlinelibrary.wiley.com/doi/pdf/10.1049/rpg2.12216>. URL: <https://ietresearch.onlinelibrary.wiley.com/doi/abs/10.1049/rpg2.12216>.
- [19] Xuesong Tang et al. “Active Power Control of Wind Turbine Generators via Coordinated Rotor Speed and Pitch Angle Regulation”. In: *IEEE Transactions on Sustainable Energy* 10.2 (2019), pp. 822–832. DOI: [10.1109/TSTE.2018.2848923](https://doi.org/10.1109/TSTE.2018.2848923).
- [20] Ana Fernández-Guillamón et al. “Power systems with high renewable energy sources: A review of inertia and frequency control strategies over time”. In: *Renewable and Sustainable Energy Reviews* 115 (2019), p. 109369. ISSN: 1364-0321. DOI: <https://doi.org/10.1016/j.rser.2019.109369>. URL: <https://www.sciencedirect.com/science/article/pii/S1364032119305775>.